



## Review

# 3D frameworks in composite polymer Electrolytes: Synthesis, Mechanisms, and applications

Lulu Du <sup>a</sup>, Bo Zhang <sup>b</sup>, Xiaofang Wang <sup>a</sup>, Chenhui Dong <sup>a</sup>, Liqiang Mai <sup>a,c</sup>, Lin Xu <sup>a,c,\*</sup>

<sup>a</sup> State Key Laboratory of Advanced Technology for Materials Synthesis and Processing, School of Material Science and Engineering, Wuhan University of Technology, Wuhan 430070, PR China

<sup>b</sup> International School of Materials Science and Engineering, Wuhan University of Technology, Wuhan 430070, PR China

<sup>c</sup> Foshan Xianhu Laboratory of the Advanced Energy Science and Technology Guangdong Laboratory, Xianhu Hydrogen Valley, Foshan 528200, Guangdong, PR China

## ARTICLE INFO

## Keywords:

Composite polymer electrolytes  
3D frameworks  
Synthesis strategies  
Ionic conductivity  
Solid-state lithium metal batteries

## ABSTRACT

Solid-state lithium metal batteries (LMBs) show promising prospects due to the high energy density and high safety. Developing novel solid electrolytes with high performance is of great significance for practical application of LMBs. Among all kinds of solid electrolytes, composite polymer electrolytes (CPEs) consisting of inorganic fillers and polymer electrolytes have drawn increasing focus because of their improved ionic conductivity and mechanical strength. However, the incompatibility between the inorganic fillers and organic polymer matrix leads to randomly distributed fillers, inevitably causing discontinuous ion transport and insufficient mechanical strength. Besides, the heavy fillers tend to aggregate and precipitate in the polymer matrix, leading to monolithic blocks for continuous ion transport. Herein, introducing ion-conducting 3D frameworks into polymer electrolytes is an effective strategy to provide continuous ion transport and mechanical support. The advances of 3D frameworks for CPEs are summarized in this review. For example, the structural design and synthesis methods of 3D frameworks and the mechanisms of ionic conductivity improvement are discussed in detail. Furthermore, some important works of the 3D frameworks in CPEs for solid-state LMBs are presented. Finally, the challenges and directions of high-performance CPEs in future research are prospected.

## 1. Introduction

Considerable attention has focused on high-energy and high-efficiency energy storage devices, due to ever-rising demands of technological products from portable devices to electric vehicles, and diminishing renewable resources over the years. Lithium-ion batteries have obtained unprecedented significance in many fields, owing to their low self-discharge rate, high energy density and long cycle life [1]. However, the energy density of commercial lithium-ion batteries with liquid electrolytes is restricted within 260 Wh kg<sup>-1</sup>, which fails to meet the high-energy requirements [2]. Therefore, exploiting novel lithium-storage batteries with high energy density is a fundamental target. In recent years, lithium metal has gained considerable attention as a promising anode material due to its distinguishing superiority, including ultrahigh theoretical specific capacity (3860 mAh g<sup>-1</sup>) and exceedingly low potential (3.040 V vs standard hydrogen electrode) [3,4]. Unfortunately, lithium dendrite growth on Li anode may penetrate the

separator and subsequently result in short circuit, which will quickly heat up the cells and cause thermal runaway. The lithium dendrite issues severely limit the large-scale commercialization of lithium metal batteries [5,6]. On the other hand, conventional liquid electrolytes usually contain flammable organic component, which poses a threat to leakage and fire hazard, and causes adverse impact on the application of lithium metal batteries. Another drawback is that liquid electrolytes are not compatible with high-voltage electrodes, thus limiting the enhancement of energy density. Because of the electrolyte solvation structure and Li<sup>+</sup> desolvation process in liquid electrolytes, highly reactive free solvents are formed on the surface of electrodes. And these highly reactive free solvents are easily oxidized and decomposed, which leads to the narrow voltage window of conventional liquid electrolytes [7].

Accordingly, development of solid electrolytes to replace liquid electrolytes is a promising strategy to address the above-mentioned issues. An effective way to hinder Li dendrite penetration is to employ mechanically robust solid electrolytes to suppress lithium dendrite

\* Corresponding author at: State Key Laboratory of Advanced Technology for Materials Synthesis and Processing, School of Material Science and Engineering, Wuhan University of Technology, Wuhan 430070, PR China.

E-mail address: [linxu@whut.edu.cn](mailto:linxu@whut.edu.cn) (L. Xu).

<https://doi.org/10.1016/j.cej.2022.138787>

Received 16 June 2022; Received in revised form 8 August 2022; Accepted 22 August 2022

Available online 24 August 2022

1385-8947/© 2022 Published by Elsevier B.V.

growth and penetration. In addition, nonflammable solid electrolytes can reduce the fire risk and avoid leakage. Moreover, solid electrolytes with expanded electrochemical window are not only able to match high-voltage cathode materials to achieve higher energy density, but also have better compatibility with lithium metal anodes [8–10].

In general, solid electrolytes include inorganic ceramic electrolytes (ICEs) and solid polymer electrolytes (SPEs). In terms of ICEs, they commonly display high ionic conductivity ( $10^{-4} \sim 10^{-3} \text{ S cm}^{-1}$ ) and wide electrochemical window. Nonetheless, their preparation process is usually time-consuming and needs high temperature, which limits the practical application. Another issue is the poor interfacial contact with electrodes, which can be attributed to their rigid and brittle nature, leading to large interface impedance and degrades the battery performance [11–13]. Conversely, SPEs are featured with close interface contact with electrodes, satisfactory flexibility as well as processing advantages. The close interface contact minimizes the interface impedance between electrolytes and electrodes. Besides, the satisfactory flexibility of SPEs holds great promise for wide applications like flexible energy storage devices. And it is worth noting that the facile processability makes it possible to control the thickness and realize large-scale manufacture. In spite of above-mentioned advantages, SPEs commonly suffer from inferior conductivity ( $<10^{-5} \text{ S cm}^{-1}$ ) at room temperature, hence extremely hampering their practical application. Apart from this, their poor mechanical strength fails to effectively suppress Li dendrite growth and further increases the possibility of safety problems [14–19]. To develop high-performance solid polymer electrolytes for practical application, some key requirements are called for design and fabrication of SPEs with excellently comprehensive properties as follows [20].

1. Dissolution ability. Solid polymer electrolytes can be obtained by dissolving Li salts into the polymer matrix, and  $\text{Li}^+$  can transport along the coordination with some polar functional groups in polymer chains, such as  $\text{CH}_2\text{-CH}_2\text{-O}$ ,  $\text{C=O}$ ,  $\text{CH}_2\text{-CF}_2$  and  $\text{C}\equiv\text{N}$ .
2. Electrochemically stability. The voltage window should be over 4 V, which is important for high energy-density energy storage devices.
3. Ionic conductivity and ion transference number. Acceptable ionic conductivity ( $\geq 10^{-4} \text{ S cm}^{-1}$  at room temperature) and ion transference number ( $\geq 0.4$ ) are required to reduce ohmic polarization and guarantee efficient rate capability in charging and discharging process.
4. Thermal stability. High thermal stability of SPEs for wide-range temperatures is essential to enable safe operation of battery.
5. Mechanical strength. Two key parameters are tensile strength and Young modulus. Tensile strength of SPEs needs to reach up to 30 MPa in order to completely separate anode and cathode. At the same time, necessary Young modulus ( $\geq 6 \text{ GPa}$ ) can resist the dendrite growth for safe batteries.
6. Electrical insulation. Electronically insulating demand for SPEs helps to minimize self-discharge process and achieve long life-span.

Diverse strategies are explored to modify SPEs for practical requirements. One is to form block copolymer or crosslinked polymers, which can enhance room-temperature conductivity to  $10^{-5} \text{ S cm}^{-1}$ , but still far from practical implementation [21–23]. Besides, introducing organic plasticizers into SPEs can considerably increase the ionic conductivity, whereas compromises mechanical properties and increases the safety risk due to the flammable plasticizers [24–25]. Another method is to disperse ceramic fillers in the polymer matrix. In this way, both of the ionic conductivity and mechanical properties of SPEs could be improved to some degree. Generally, the ceramic fillers can be non-Li-conducting fillers, including  $\text{Al}_2\text{O}_3$  [26],  $\text{SiO}_2$  [27],  $\text{ZrO}_2$  [28], and Li-conducting fillers, like  $\text{Li}_3\text{xLa}_{2/3-\text{x}}\text{TiO}_3$  (LLTO) [29],  $\text{Li}_7\text{La}_3\text{Zr}_2\text{O}_{12}$  (LLZO) [30],  $\text{Li}_{1+\text{x}}\text{Al}_\text{x}\text{Ti}_{2\text{x}}(\text{PO}_4)_3$  (LATP) and  $\text{Li}_{1+\text{x}}\text{Al}_\text{x}\text{Ge}_{2\text{x}}(\text{PO}_4)_3$  (LAGP) [31], etc. However, these randomly distributed ceramic fillers in powder form fail to supply long-range and continuous Li-ion conduction pathways, which in turn lead to limited enhancement of ionic conductivity.

Recently, Cui group [32] have reported that ceramic nanowires with high aspect ratio could provide extended ion-conducting channels, which contributes to the higher ionic conductivity compared to nanoparticle fillers. However, the enhancement of the ionic conductivity is limited owing to the agglomerated ceramic nanowires in the polymer matrix. To overcome the agglomeration issue, in situ preparation of highly monodispersed nanoparticles as fillers for polymer-based electrolytes has been reported. Because of the isolated  $\text{SiO}_2$  nanoparticles in the polymer matrix, the ionic conductivity of the composite electrolyte was only  $4.4 \times 10^{-5} \text{ S/cm}$  at  $30^\circ\text{C}$ , which is far from the standard for practical application [33].

Generally, there has been an ionic conductivity vs mechanical strength dilemma in polymer electrolytes. Satisfying ionic conductivity usually needs lower crystallization to promote the segmental motion of the polymer for rapid ion conduction [34]. However, lower crystallization deteriorates the mechanical strength of the SPEs and compromises the battery safety. To address this dilemma, design and construction of versatile 3D frameworks applied in SPEs is an effective strategy to obtain high-performance CPEs with both high mechanical properties and high ionic conductivity. The versatile 3D frameworks can not only provide continuous and long-range ion transport pathways, but also avoid the filler agglomeration and precipitation in the polymer matrix, which contributes to the highly improved ionic conductivity. Furthermore, the 3D frameworks can considerably boost the mechanical strength of the CPEs, which can suppress the dendrite formation and growth [35].

More importantly, the synergetic effect of soft polymer matrix and mechanically robust 3D frameworks could be  $1 + 1 > 2$ , which opens a new avenue for high-performance solid electrolytes with superior comprehensive properties such as excellent electrochemical performance, good mechanical strength, and high-safety nature. Up to now, several types of 3D frameworks have been applied in CPEs, which can be summarized and classified into four main categories: bi-continuous ordered 3D frameworks, vertically aligned 3D frameworks, interconnected fiber 3D frameworks and porous hydrogel/aerogel 3D frameworks, as shown in Fig. 1. Benefiting from the brilliant design of these 3D frameworks, the composite polymer electrolytes with versatile 3D frameworks show higher ionic conductivity, wider electrochemical window, stronger mechanical strength and higher safety.

In this review, we present the structure design and synthesis methods according to the categories of 3D frameworks. Then, the possible mechanisms of ionic conductivity enhancement are discussed. Furthermore, based on the structural and compositional features of the 3D frameworks, we introduce some significant advances applied in composite solid electrolytes for solid-state lithium batteries. Finally, we propose the significance and challenges of 3D frameworks for solid-state lithium batteries.

## 2. Structure design and fabrication of 3D frameworks in CPEs

A composite polymer electrolyte with a unique 3D framework is a promising strategy to obtain high-performance solid electrolytes with fast ion conduction and high mechanical strength. When constructing the unique 3D frameworks, the design and synthesis approach is of great importance. For this reason, we are going to begin with the prominent fabrication methods of the 3D frameworks prior to discussing their mechanism and wide application in CPEs. As shown in Fig. 2, four dominant approaches are schematically described, such as template method, 3D printing method, electrospinning method and hydrogel-derived method, and each one will be described in detail as follows.

### 2.1. Template method

Ice-template method is a simple but effective template method for fabricating 3D frameworks, which uses ice as the sacrificing template. In the process, a starting aqueous suspension containing uniformly

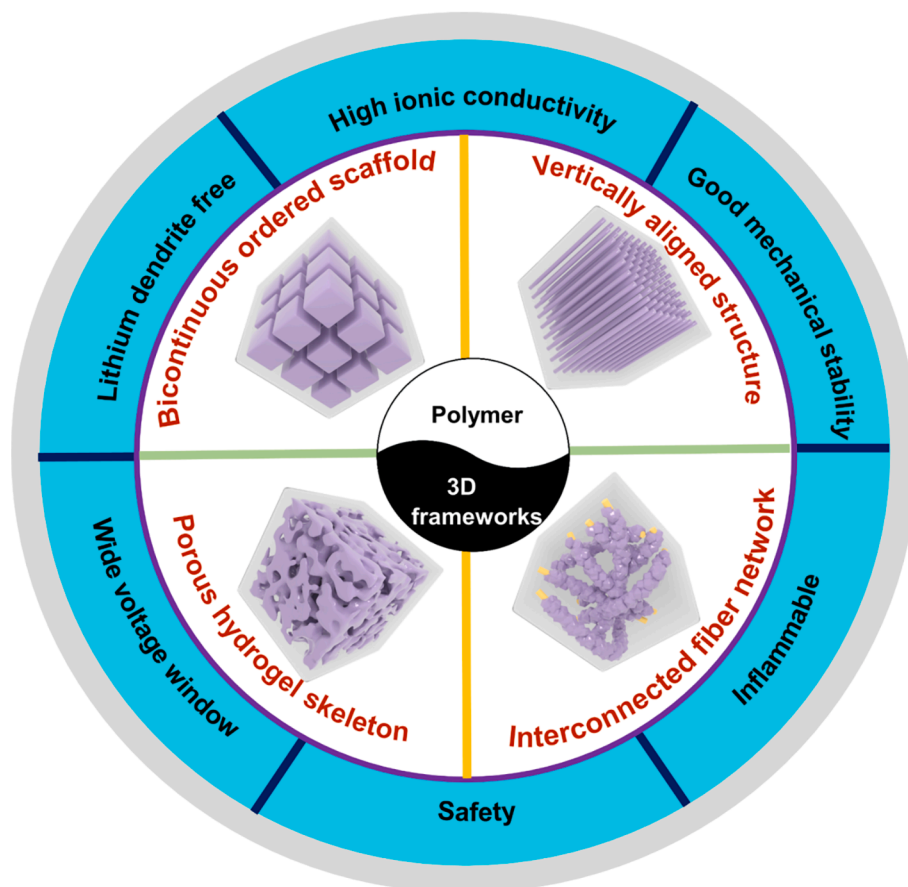


Fig. 1. Versatile 3D frameworks applied in CPEs and the advantages of the CPEs with 3D frameworks.

dispersed nanoparticles needs to be placed on a cold finger with low temperature. In this way, the bottom of the suspension is cooled at first to form a vertical temperature gradient. Therefore, ice crystal grows from the bottom and pushes nanoparticles to the side, after removing the ice, 3D vertical frameworks can be obtained. Because ice is commonly selected as the template, this method is an environmentally friendly and low-cost approach, which has been applied to fabricate desirable 3D vertical frameworks for CPEs. Using this ice template method, Yang group [36] prepared a composite solid-state electrolyte with vertically aligned LATP framework to provide fast and continuous ion transport channels. The ionic conductivity of the electrolyte with vertically aligned LAGP framework is 6.9 times higher than that of its counterpart with randomly dispersed LAGP particles. In addition, they used the same method to fabricate another vertical 3D framework with LATP ion conductor as starting material. As expected, the similar findings are also observed in this system [37]. Accordingly, ice-template method is a facile and effective way to design 3D vertical frameworks for CPEs with fast ion transport pathways and good mechanical strength. The final structure can be tailored via adjusting the concentration of the nanoparticles, cooling rates and sintering parameters.

Other templates also have been applied to design and fabricate the 3D frameworks for CPEs such as bacteria cellulose and natural wood. The common process of the template method has three steps: (1) pre-treatment of templates; (2) impregnation of templates with precursor solutions; (3) conversion of precursors into final products. The template method is a simple and low-cost technology to obtain necessary architecture. For example, Hu group [38] proposed a facile method to construct a connected LLZO framework by using bacteria cellulose as a template. The well-organized LLZO framework was synthesized by sintering the pre-treated bacteria cellulose with LLZO precursor solution to remove the template and form the 3D structure, which inherits the

structural merit of the initial bacteria cellulose. Then, polymer electrolyte was introduced into the porous structure, serving as a protective layer to enhance the mechanical resilience of this network. Due to the continuous lithium-ion transport paths, the ionic conductivity of the CPEs can be improved to  $1.12 \times 10^{-4} \text{ S cm}^{-1}$ . Inspired by the unique structure of natural wood, the wood was used as a sacrificial template to prepare a garnet skeleton with vertically aligned structure. The original wood was pre-treated by a compression process, followed by filling the garnet precursor into vertical channels. Finally, the garnet precursor was transferred into garnet framework with the assistance of calcination. The as-fabricated garnet backbone with low tortuosity can provide unobstructed  $\text{Li}^+$  conductive pathways [39]. These works provide a new idea to construct 3D frameworks for composite polymer electrolytes via a template method.

## 2.2. 3D printing method

3D printing, a disruptive manufacturing technology, is rising as an innovative and facile method to design and fabricate unique structures compared to traditional material preparation methods [40–42]. 3D printing shows some main advantages: (1) It presents remarkable processing flexibility and geometry controllability; (2) The material thickness could be well controlled due to the layer-by-layer additive processing nature; (3) It has been considered as a facile and effective method because of its one-step process. Thereby, increasing attention has been paid to the fabrication of solid-state electrolytes with fine 3D frameworks by the 3D printing method. For instance, Hu group [43] proposed “brick-and-mortar” strategy for a composite solid electrolyte membrane by a 3D printing method, and the preparation process of the “brick-and-mortar” composite solid electrolyte can be seen in Fig. 2b. The LLZO membrane was diced into square chips and the was tightly

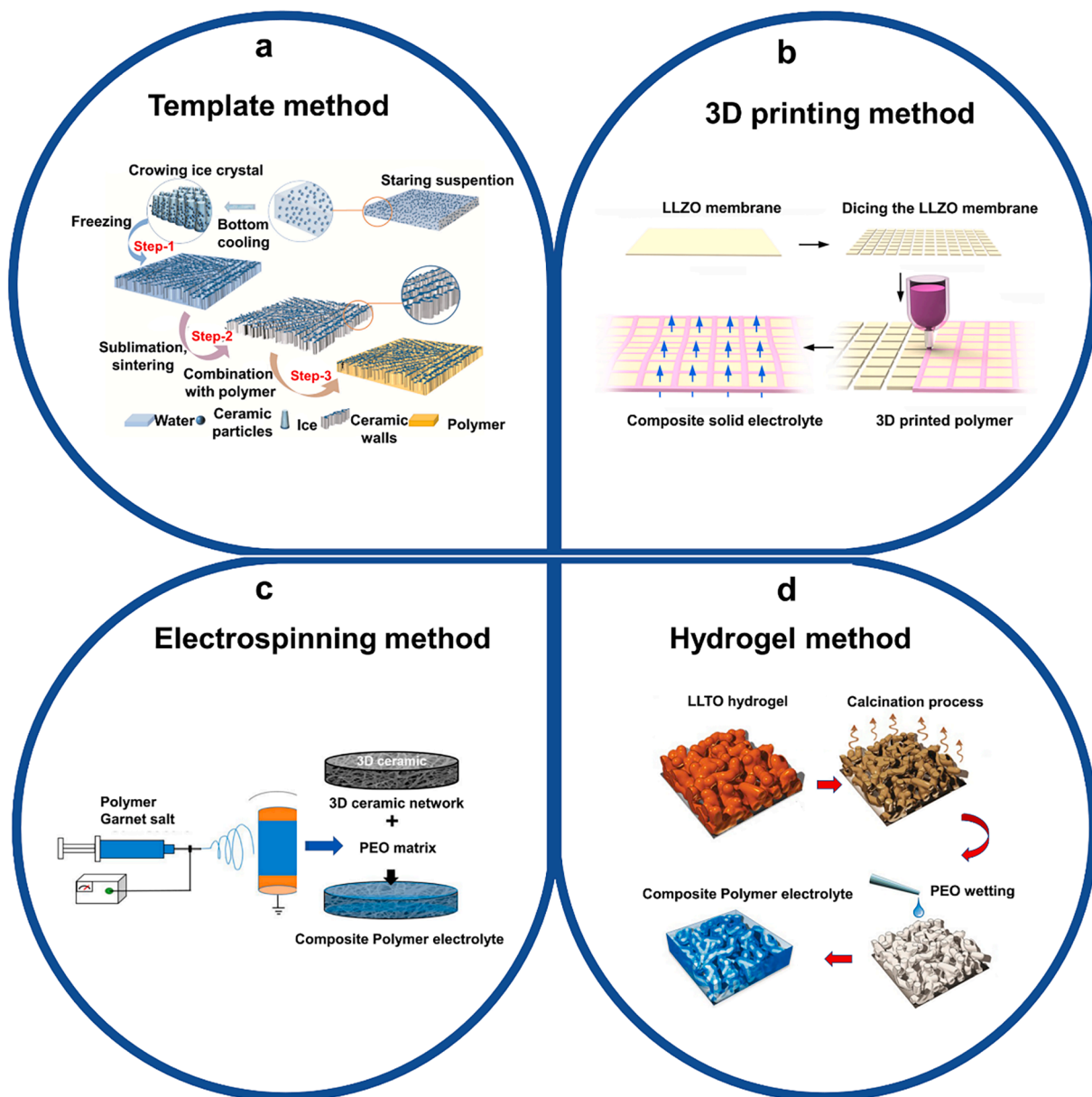


**Fig. 2.** Fabrication methods of 3D frameworks for CPEs. (a) Template method. Reprinted with permission.[37] Copyright 2019, Elsevier. (b) 3D printing method. Reprinted with permission.[43] Copyright 2019, American Chemical Society. (c) Electrospinning method. Reproduced with permission.[53] Copyright 2016, National Academy of Sciences. (d) Hydrogel method. Reprinted with permission.[55] Copyright 2019, Wiley-VCH.

connected by the polymer binder extruded from a 3D printer nozzle. The brick-like LLZO chips can provide fast ion-conducting paths, while the polymer binder endows the resulting composite solid electrolyte with great flexibility, which can release the strain caused in preparation process, packaging process, transportation process and application. Besides, Bruce group [44] prepared a composite solid electrolyte with 3D bi-continuous ordered ceramic and polymer microchannels by a 3D printing method which can precisely control the microstructures of the LAGP skeleton. The obtained CPEs deliver a higher ionic conductivity and higher mechanical strength compared with the conventional ceramic solid electrolytes. Those works inspire us that 3D printing method is promising to fabricate favorable 3D frameworks for CPEs which can not only possess remarkable mechanical performance, but also deliver desirable ionic conductivity.

### 2.3. Electrospinning method

Electrospinning method is commonly considered as an effective technology to synthesize unique interconnected fiber networks. To obtain desired 3D fiber networks, many research efforts have been dedicated to modify the electrospinning method which usually includes preparation of precursor solution process, electrospinning process and sintering process [45–47]. In comparison with other synthesis approaches, each process in electrospinning method can be easily controlled. When preparing the precursor solution, it is easy to adjust the viscosity and concentration of the solution via altering the ratio of polymer matrix and ceramics, which has an important impact on the architecture of the final 3D frameworks. In the electrospinning process, receiving length, voltage and the diameter of needles all can be controlled to tailor the structure of the 3D frameworks. And in the sintering process, polymers with different thermal properties may result in different morphologies and structures of the resultant 3D frameworks

[48–52]. Many successful CPEs with 3D fibrous frameworks have been prepared by the electrospinning method. For instance, Hu group [53] prepared a 3D  $\text{Li}_{6.4}\text{La}_3\text{Zr}_2\text{Al}_{0.2}\text{O}_{12}$  (LLZO) network by an electrospinning method as an advanced filler for composite polymer electrolytes as shown in Fig. 2c. In this structure, the 3D LLZO network can enable continuous ion transport and simultaneously enhance the mechanical strength of the CPE. Afterwards, using a sol–gel electrospinning method, Yu group [54] designed a mesoporous  $\text{Li}_2\text{SO}_4$ -modified  $\text{SiO}_2$  nanofiber network to promote pure polymer electrolytes, in which  $\text{Li}_2\text{SO}_4$  can be in situ introduced into the  $\text{SiO}_2$  nanofiber network. The introduction of  $\text{Li}_2\text{SO}_4$  in the  $\text{SiO}_2$  nanofiber network endows the inert  $\text{SiO}_2$  with ion-conducting capacity. And the mesoporous surface of the  $\text{Li}_2\text{SO}_4$ -modified  $\text{SiO}_2$  nanofiber network enhances the wettability between the composite network and PEO matrix for intimate contact, which not only enhances the mechanical properties of the final composite electrolyte, but also contributes to the improved electrochemical stability. After filling the PEO matrix into the hierarchical  $\text{Li}_2\text{SO}_4$ -modified  $\text{SiO}_2$  nanofiber skeleton, the as-obtained composite solid electrolyte shows an improved ionic conductivity. These intriguing results indicate that the electrospinning method has great potential for fabrication of interconnected fiber 3D frameworks.

#### 2.4. Hydrogel-derived method

Designing a 3D percolated hydrogel-derived framework has been considered as a fascinating method to avoid filler agglomeration and form continuous pathways for ion transport at high filler concentration in polymer matrix. The percolated networks have tunable hierarchical structures and interconnected channels for fast ion conduction. And the preparation process of the 3D percolated frameworks by the hydrogel-derived method is quite simple, which will be introduced in detail as follows. Commonly, the preparation process of the 3D nanostructured hydrogel-derived hydrogel has two steps. One is to prepare the 3D ceramic hydrogel. To be specific, ceramic precursors are dispersed in polymer solution, and then the mixture began to gelate with the assistance of cross linker and initiator to form a hydrogel. The second step is to sinter the as-obtained hydrogel to obtain 3D percolated frameworks. Using the hydrogel-derived method, Yu group [55] transformed randomly dispersed LLTO particles into a continuous 3D framework and applied it in composite polymer electrolyte (Fig. 2d), which delivers a high ionic conductivity of  $8.8 \times 10^{-4} \text{ S cm}^{-1}$  at room temperature. And the assembled full solid-state batteries exhibit excellent electrochemical and mechanical properties. Afterwards, the same group developed another hydrogel-derived framework by using LLZO as precursor, which connects the scattered LLZO nanoparticles to form a porous 3D percolated framework. The continuous garnet structure provides fast ion transport pathways without barriers, and the introduction of PEO matrix enables the composite solid electrolyte with good flexibility [56]. Thus, the hydrogel-derived method provides an effective strategy to prepare 3D frameworks for high-performance solid-state electrolytes.

In conclusion, 3D frameworks with different structures need different fabrication methods. For example, ice-template method is a simple but effective template method for fabricating 3D frameworks with vertically aligned structure by a vertical temperature gradient. 3D printing method is commonly used to fabricate 3D bi-continuous ordered frameworks due to the highly controlled process of the 3D printing technology. The electrospinning method has great potential for fabrication of interconnected fiber 3D frameworks. And the hydrogel-derived method is a quite simple and efficient strategy to form a porous 3D percolated framework. Despite the above-mentioned 3D frameworks can be obtained, precise control of 3D frameworks with well-ordered structure still remains a challenge. Besides, novel strategies and advanced technology should be developed for constructing favorable 3D frameworks.

### 3. Ion transport mechanisms of CPEs

It is highly significant to understand the Li-ion transport mechanisms in CPEs for fabricating high-performance solid electrolytes with practical applied value. CPEs consist of polymer matrix and incorporated fillers, thus the ion conduction capability of the polymer matrix and incorporated fillers has a great impact on comprehensive properties of the CPEs.

#### 3.1. Ion transport mechanism in polymer matrix

Polymer solid electrolytes can be obtained by dissolving Li salts into the polymer matrix. Particularly, Li salts dissolved in polymer electrolytes should possess low lattice energy in order to dissociate  $\text{Li}^+$  ions. In polymer-based electrolytes,  $\text{Li}^+$  can transport along the coordination with some polar functional groups in polymer chains, such as  $[-\text{CH}_2-\text{CH}_2-\text{O}-]$  in poly(ethylene oxide) (PEO),  $[\text{C}=\text{O}]$  in poly(methyl methacrylate) (PMMA),  $[-\text{CH}_2-\text{CF}_2-]$  in poly(vinylidene fluoride) (PVDF) and  $[\text{C}\equiv\text{N}]$  in polyacrylonitrile (PAN) as shown in Fig. 3a [57]. Continuous segmental motion in polymer chains produce free volume which helps  $\text{Li}^+$  transport from one coordination site to another or hop from one chain to another. As shown in Fig. 3a, the polar sequential  $[-\text{O}-]$  in PEO chains facilitates to dissociate lithium salts and generate more free  $\text{Li}^+$  ions [58]. In addition, another possible Li-conducting pathway is its macromolecular structures due to the flexible chain in PEO [59]. Nevertheless, pure PEO solid electrolytes display limited ionic conductivity of  $10^{-7} \text{ S cm}^{-1} \sim 10^{-6} \text{ S cm}^{-1}$  because of their high degree of crystallization [60]. The effective  $\text{Li}^+$  ions transport mainly occurs in amorphous phase in PEO. Besides, the  $[\text{C}\equiv\text{N}]$  in PAN can interact with Li salts, and  $\text{Li}^+$  ions can transport in PAN by moving to electron rich groups. The  $[\text{C}\equiv\text{N}]$  in PAN makes this polymer possesses a strong electron withdrawing ability, thus endowing PAN-based polymer electrolytes with a low LUMO and great electrochemical stability, which results in a wide voltage window for PAN-based polymer electrolytes [61,62]. As we all known,  $\text{Li}^+$  ions mainly diffuse in the amorphous region. Thus, it is vital for polymer electrolytes with low crystallization to achieve high ionic conductivity. PMMA is a kind of polymer whose amorphous phase is a dominant composition at relatively low temperature. Li ions transport can be achieved with assistance of break/formation of coordination between  $[\text{C}=\text{O}]$  in PMMA and Li salts [63,64]. Another common polymer electrolyte is PVDF, a semicrystalline polymer with electrical dipoles in the polymeric chain  $[-\text{CH}_2-\text{CF}_2-]$ , which endows PVDF with high dielectric constant [65,66]. The high dielectric constant is important for polymer solid electrolytes to avoid conduction of electrons, thereby helping separate Li salts for more free  $\text{Li}^+$  ions.

#### 3.2. Ion transport mechanism in Li-conducting fillers

The other important component in CPEs is incorporated fillers, which can be divided into inert fillers and active fillers. Inert fillers cannot intrinsically transport Li ions, whereas active fillers are intrinsic ionic conductors. The commonly used active fillers are perovskite-type, NASICON-type, garnet-type and sulfide-type ceramics [67]. For these ionic conductors, ion transport relies on mobile vacancies or interstitial ions, which contributes to the high ionic conductivity. In detail, perovskite-type ICEs possess a typical structure of  $\text{ABO}_3$  (A=La, Sr, or Ca; B=Al or Ti) as shown in Fig. 3b, where Li can be doped at A site to form  $\text{Li}_{3x}\text{La}_{2/3-x}\text{TiO}_3$  (LLTO) with a high ionic conductivity at room temperature [68]. However, the reduction of  $\text{Ti}^{4+}$  to  $\text{Ti}^{3+}$  with lithium metal anode can improve the electronic conductivity and decomposition of the ICEs, which limit their further applications for solid lithium metal batteries [69].

NASICON-type ICEs have a common structure of  $\text{NaM}_2(\text{PO}_4)_3$  (M=Ti, Ge, or Zr), which were first developed as  $\text{Na}^+$  ion conductors [70]. After replacement of  $\text{Na}^+$  with  $\text{Li}^+$ , these types of ICEs possess Li-conducting ability with similar crystal structure of  $\text{NaM}_2(\text{PO}_4)_3$ . Unfortunately,

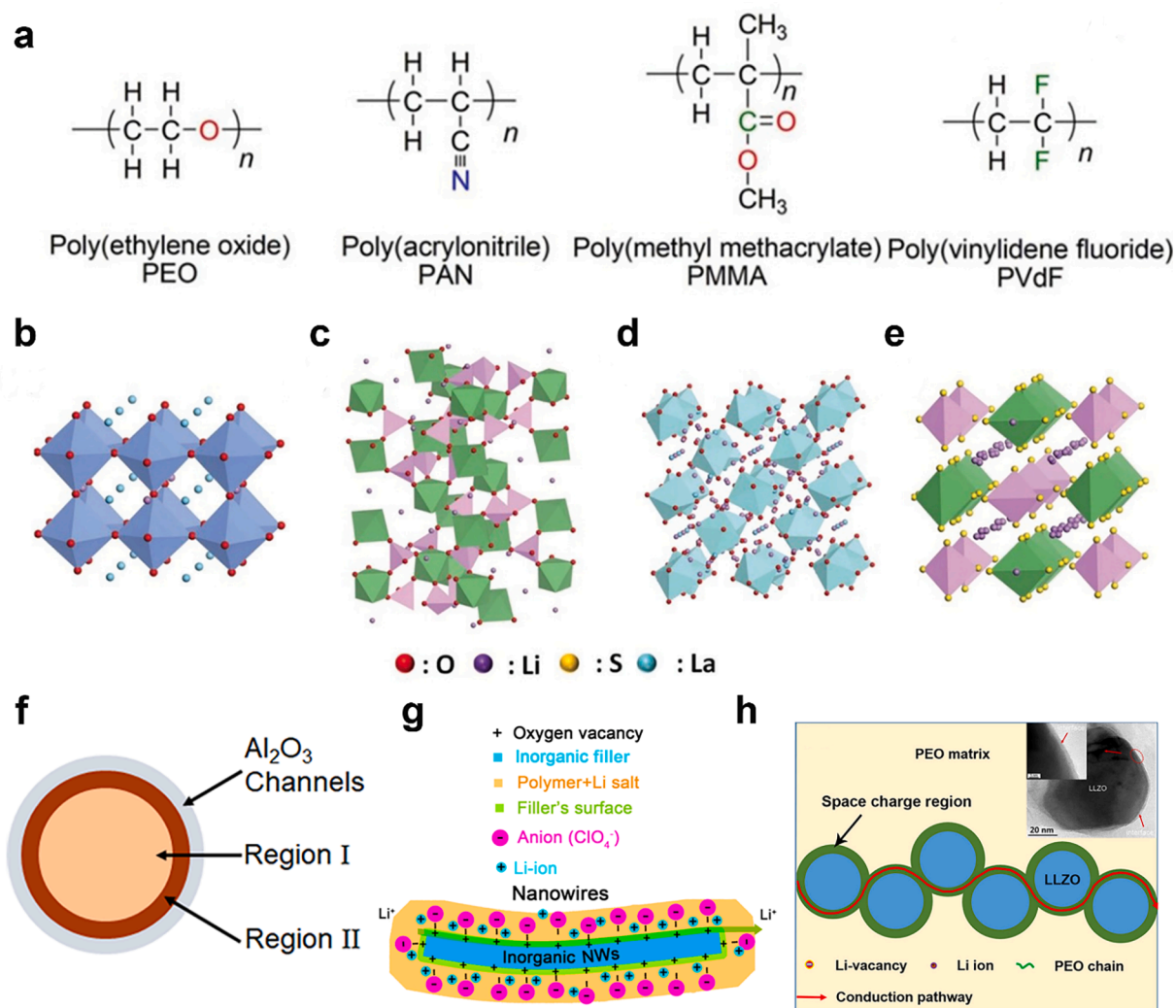


**Fig. 3.**  $\text{Li}^+$  ions transport mechanism in CPEs. (a) The chemical structures of commonly used polymer matrices for CPEs. Reprinted with permission. [57] Copyright 2018, Electrochemical Society. The crystal structures of (b) Perovskite-type ceramics. (c) NASICON-type ceramics. (d) Garnet-type ceramics. (e) Sulfide-type ceramics. Reprinted with permission. [67] Copyright 2018, Wiley-VCH. (f) Schematic of polymer electrolytes in nanochannel of the Lewis acid-modified AAO. Reprinted with permission. [84] Copyright 2018, American Chemical Society. (g) Schematic of  $\text{Li}^+$  transport along the interface between polymer matrix and fillers rich in oxygen vacancies on the surface. Reprinted with permission. [32] Copyright 2015, American Chemical Society. (h) Schematic illustration of the fast ion conduction pathways along the space charge regions and TEM images of the Ga-LLZO/PEO interface. Reprinted with permission. [89] Copyright 2019, American Chemical Society.

the ion replacement compromises the conductive ability of the NASICON-type ICEs. In order to address this challenge, two main NASICON-type ICEs of  $\text{Li}_{1+x}\text{Al}_x\text{Ti}_{2-x}(\text{PO}_4)_3$  (LATP) and  $\text{Li}_{1+x}\text{Al}_x\text{Ge}_{2-x}(\text{PO}_4)_3$  (LAGP) are designed by partly substituting Al. After doping of Al, the NASICON-type ICEs can display an ionic conductivity as high as  $10^{-3} \text{ S cm}^{-1}$  [71,72]. On the other hand, NASICON-type ICEs suffer from the same challenge of the poor compatibility with lithium metal anodes owing to the reduction of  $\text{Ti}^{4+}$  to  $\text{Ti}^{3+}$  with Li metal.

Garnet-type ICEs can be expressed as  $\text{A}_3\text{B}_2(\text{XO}_4)_3$  ( $\text{A}=\text{Ca}, \text{Mg}, \text{Y}, \text{or La}$ ;  $\text{B}=\text{Al}, \text{Fe}, \text{Ga}, \text{Ge}, \text{Mn}, \text{Ni}, \text{or V}$ , and  $\text{X}=\text{Si}, \text{Ge}, \text{or Al}$ ). Currently, one of the most popular garnet-type ICEs is  $\text{Li}_7\text{La}_3\text{Zr}_2\text{O}_{12}$  (LLZO) as shown in Fig. 3d, which presents an ionic conductivity up to  $10^{-4} \text{ S cm}^{-1}$  at room temperature and wide electrochemical window more than 4.5 V. Unlike LATP and LLTO, LLZO possesses excellent chemical stability with lithium metal anodes because of its intrinsic inert towards lithium metal. Moreover, the ionic conductivity of garnet-type LLZO ICEs could be enhanced after aliovalent replacement of La or Zr with some elements like Ga, Nb, and Ge [73–76]. Although garnet-type LLZO ICEs can display ideal ionic conductivity and superior compatibility with lithium metal anode, Li dendrite growth and poor interface contact with

electrodes restrict their further development in solid battery fields.

Sulfide-type ICEs (Fig. 3e) show great potential in solid electrolytes due to their higher ionic conductivity ( $10^{-3} \sim 10^{-2} \text{ S cm}^{-1}$ ) and wider electrochemical window.  $\text{Li}_{10}\text{GeP}_2\text{S}_{12}$  (LGPS), as one of the typical sulfide-type ICEs, can present a room-temperature ionic conductivity as high as  $1.2 \times 10^{-2} \text{ S cm}^{-1}$  [77]. However, among the raw materials for preparation of LGPS ICEs,  $\text{GeS}_2$  is a kind of high-cost material [78]. Another drawback is that sulfide-type ICEs are unstable with moisture in air, which induces hydrolyzation of sulfides and consequent generation of  $\text{H}_2\text{S}$  gas [79]. These disadvantages hence hamper the practical applications of sulfide-type ICEs for solid LIBs.

The commonly used inorganic ceramic fillers for composite polymer electrolytes are in powder form, which are prone to aggregate because of the poor compatibility between the inorganic ceramic fillers and organic polymer matrix. In addition, these incorporated inorganic ceramic fillers are readily precipitated owing to the larger weight during the film-forming process. The aggregation and precipitation issue are long-standing challenges for continuous  $\text{Li}^+$  transport. Another drawback is that the incorporated inorganic ceramic fillers are randomly distributed in the polymer matrix, which fails to supply long-range and continuous

Li-ion conduction pathways. In contrast, ceramic 3D frameworks can not only provide continuous and long-range ion transport pathways, but also avoid the filler agglomeration and precipitation in the polymer matrix, which contributes to the highly improved ionic conductivity.

### 3.3. Ion transport mechanism in polymer/filler interface

In addition to aforementioned Li-conducting mechanisms in CPEs, fast ion transport can be achieved in the polymer/filler interface. The incorporated fillers (both active and inactive fillers) serve as solid plasticizers to enhance the ionic conductivity for polymer electrolytes. The nanosized fillers with large surface area can reduce the crystallinity of polymer matrix near the filler/polymer interface and form more amorphous regions, which facilitates the motion of polymer chains and further promotes the ion conduction [80,81]. Besides, the Lewis acid-base interactions between surface groups of fillers and anionic ions mainly contribute to the fast Li<sup>+</sup> conduction interface. Some acidic groups on the filler surface behave as Lewis acid center, and can absorb the anionic ions in polymer matrix, which facilitates the Li salts dissociation and hence releases more free Li ions [82,83]. This mechanism has been proven through experiment by Cui group (Fig. 3f). They fabricated a novel composite electrolyte using AlF<sub>3</sub>-modified AAO as the non-conductive framework and poly(ethylene oxide) as polymer matrix. Al<sub>2</sub>O<sub>3</sub> is a kind of inert filler which fails to transport Li ions by itself. And the ionic conductivity improvement in this composite electrolyte can be attributed to the interfacial interaction derived from the PEO and AlF<sub>3</sub>-modified Al<sub>2</sub>O<sub>3</sub>. The hybrid electrolyte with pure Al<sub>2</sub>O<sub>3</sub> with vertical nanopores can deliver an ionic conductivity of  $1.79 \times 10^{-4}$  S cm<sup>-1</sup> at room temperature. In order to further promote the Li ions transport, the Al<sub>2</sub>O<sub>3</sub> was modified by a layer of AlF<sub>3</sub> which is a typical Lewis acid and can have strong Lewis acid-base interactions with Li salts to set free Li ions. After the modification of the AlF<sub>3</sub> layer, the ionic conductivity can reach up to  $3.50 \times 10^{-4}$  S cm<sup>-1</sup>, which is twice as high as that without AlF<sub>3</sub> coating [84]. All the results demonstrate that the Lewis acid-base interaction at the polymer/filler interface can facilitate the Li ions transport.

Moreover, the fast Li ions conduction at the polymer/filler interface may come from the oxygen vacancies on the surface of the incorporated fillers (Fig. 3g). In general, oxygen vacancies are beneficial for ionic conductivity enhancement [85]. The existence of the oxygen vacancies can facilitate Li ions to hop from one vacancy to another, which can form a continuous and high-speed pathway for Li ions conduction [86]. Apart from this, the oxygen vacancies on the surface of active/inert fillers result in the positive-charged surfaces, which can form a strong bond between positive-charged surfaces of inorganic fillers and the anion of the Li-salt in the polymer matrix. This promotes the Li ions mobility and enables the fast ion transport at the filler/polymer interface [32].

Another mechanism of the fast Li<sup>+</sup> conduction at the interface is the space-charge effect. Space-charge regions form when two materials with different chemical potentials being in contact, and the defects are redistributed under the driving force of potential differences [87]. To be specific, Li vacancies and Li ions are uniformly distributed in the ceramic fillers. When a second phase is introduced, like the polymer matrix, the Li ions inside the ceramic lattice sites transfer to surface sites because of the interfacial chemical potential. This migration leads to the high content of Li<sup>+</sup> and the low content of vacancies on the surface of the ceramic fillers, which facilitates the rapid ion conduction. Generally speaking, space charge regions have two common effects on solid electrolytes. One is that the defect concentration change has a great influence on ionic conduction [88]. Besides, this region offers a new kinetic path for ions transport. Recently, a surface layer of 3 nm space charge region has been observed by TEM characterization in a PEO/Ga-LLZO composite solid electrolyte (Fig. 3h). In this work, the continuous space charge region at the PEO/Ga-LLZO interface results in an improved ionic conductivity [89].

Based on above discussions, for CPEs with inactive 3D frameworks,

Li<sup>+</sup> can conduct in the polymer matrix and the interfaces between the 3D frameworks and polymer matrix. Whereas in CPEs with active 3D frameworks, Li<sup>+</sup> can transfer along the conductive 3D frameworks and polymer matrix, or their interfacial regions, which indicates that the active 3D frameworks are promising for higher ionic conductivity. There are many reports about the ionic conduction in polymer matrix and inorganic ceramic phase. However, thorough investigation on interfacial conduction mechanisms for CPEs is highly inadequate. Deeper understanding and more experimental investigation should be made on the oxygen vacancy effect and space charge effect and so on.

## 4. Applications of 3D frameworks in CPEs

High-energy and high-safety demands have stimulated the rapid development of all-solid-state LIBs with high-performance solid electrolytes. As discussed above, introduction of 3D frameworks for CPEs is an effective strategy to fabricate high-performance solid electrolytes with superior comprehensive properties such as high ionic conductivity, good mechanical strength, and excellent thermal stability, which will promote the development of solid LMBs with high energy and high safety. In this section, some selected research advances of 3D frameworks in solid lithium batteries are presented according to different types of 3D frameworks in succession.

### 4.1. Interconnected fiber 3D frameworks

#### 4.1.1. Ceramic fiber 3D frameworks

According to the shapes of the incorporated fillers in CPEs, they can be classified into 0D nanoparticles [90], 1D nanowires/nanotubes [91], 2D nanosheets and 3D frameworks [92–94]. Fabrication of 3D frameworks has been considered as an effective method to enable continuous ion transport and high mechanical strength. Among numerous 3D frameworks, interconnected fiber networks with high surface area/volume ratio are promising candidates to promote ion transport and electrochemical stability. Some important works of designing interconnected fiber 3D frameworks are introduced in this section. For example, Hu group [53] fabricated a new 3D LLZO nanofiber network for CPEs (Fig. 4a). Notably, it is the first time to design and construct a 3D ceramic network derived from garnet-type nanofibers to form continuous Li-ion transport in PEO electrolytes. The 3D LLZO network was prepared by an electrospinning method, and the composite electrolyte could be obtained by infiltration of PEO electrolyte into the porous network to completely cover the 3D LLZO nanofiber network. As a result, the ionic conductivity of the CPE is improved with the assistance of the 3D LLZO nanofiber network (Fig. 4b). In addition, the LLZO-network-reinforced solid electrolyte shows highly improved mechanical strength compared with the pure PEO electrolyte, which facilitates long-time cycling stability by effectively inhibiting lithium dendrite growth (Fig. 4c). Meanwhile, because of the flexible PEO matrix, the LLZO-network-reinforced solid electrolyte possesses excellent flexibility as well, which indicates the great promise for flexible energy storage devices. Afterwards, the same group developed a simple template method to construct the 3D LLZO network by using bacteria cellulose (BC) as a template (Fig. 4d). The well-organized LLZO network was obtained by high-temperature calcination of the pre-treated bacteria cellulose which had absorbed the LLZO precursor solution. Then, the PEO-based electrolyte was incorporated into the as-prepared porous and interconnected 3D LLZO network (Fig. 4e), which could act as a protection layer to enhance the mechanical resilience of this ceramic network. This rational design can not only address the brittleness problem of ceramic solid electrolytes, but also improve the ionic conductivity by providing continuous and long-range Li<sup>+</sup> transfer pathways (Fig. 4f) [38]. In another work, they tried to use cellulose textile as template to construct flexible Li-conducting ceramic textile. This garnet textile is composed of LLZO ion conductor, which can provide continuous Li<sup>+</sup> transfer channels and present light weight, desired flexibility and porous structure

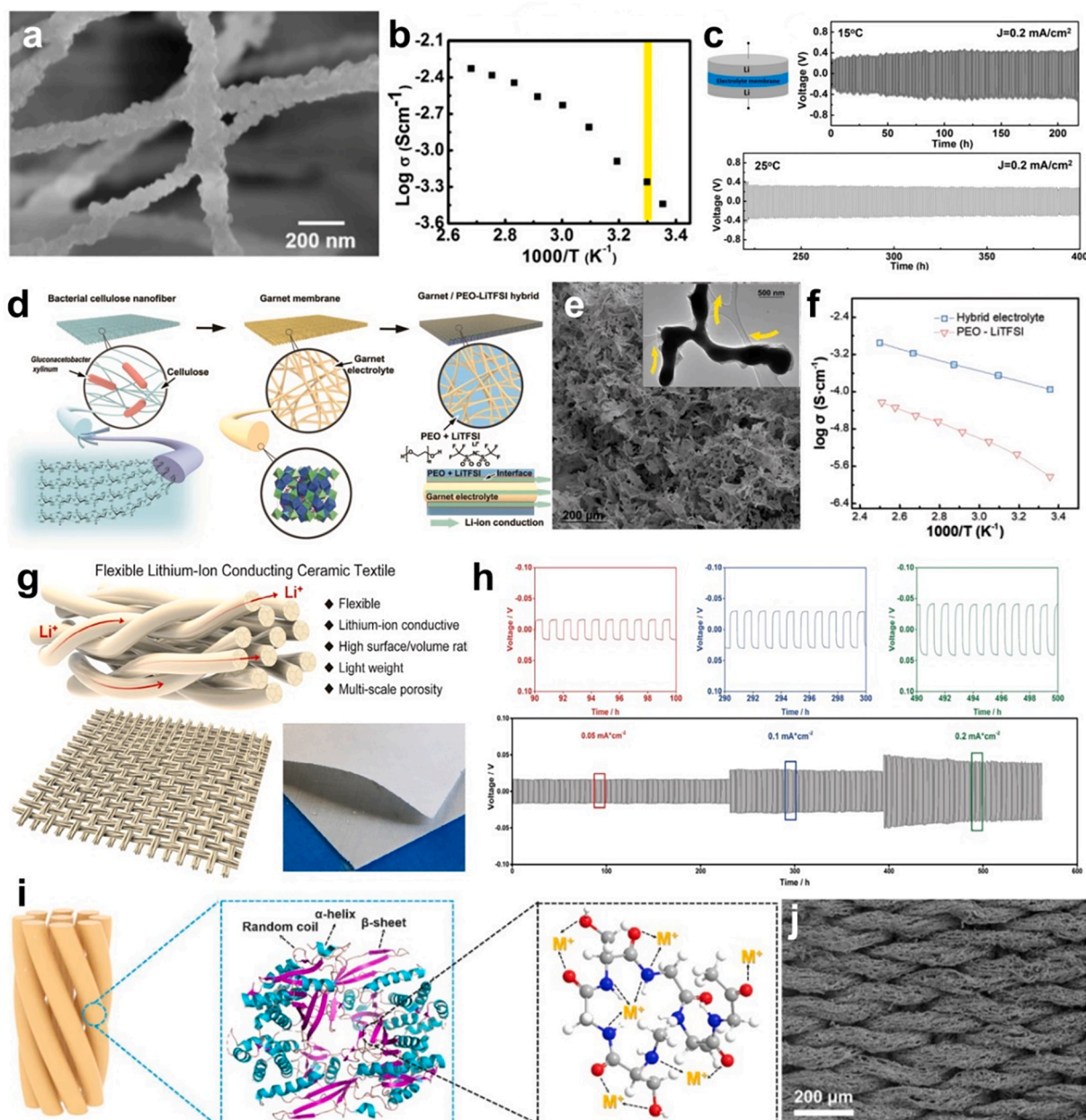


**Fig. 4.** Design of ceramic fiber 3D frameworks and their application in CPEs for LMBs. (a) SEM image of the electrospun LLZO nanofiber 3D network. (b) Arrhenius plot of the LLZO-network-reinforced CPE at elevated temperatures. (c) Electrochemical performance of the LLZO-network-reinforced CPE in symmetric Li cells. Reproduced with permission.[53] Copyright 2016, National Academy of Sciences. (d) Fabrication process of the LLZO network by using bacteria cellulose as a template and the resulting CPE. (e) SEM image of the LLZO network. Inset is the TEM image of single LLZO fiber. (f) Comparison of ionic conductivities of electrolytes with and without the LLZO network. Reprinted with permission.[38] Copyright 2018, Wiley-VCH. (g) Schematic illustration of the conducting garnet textile and the corresponding optical photograph. (h) Electrochemical performance of the garnet-textile-reinforced CPE in symmetric Li cells at different current densities. Reprinted with permission.[95] Copyright 2018, Elsevier. (i) Adsorption mechanism of metal ions on the silk fabric template. (j) SEM image of the LLZO ceramic fabric from the silk fabric template. Reprinted with permission.[96] Copyright 2022, Elsevier.

(Fig. 4g). The garnet textile was prepared by filling the LLZO precursor into the cellulose textile template coupled with calcination process to remove the template and form LLZO phase, which can inherit the structural features of pristine cellulose textile template. Then, the PEO-based electrolyte was repeatedly immersed into this ceramic textile until a dense electrolyte can be obtained. As a result, the garnet-textile-reinforced CPE displays a high ionic conductivity. During the long-term cycling tests, the assembled Li-Li cell can be stable without short circuit, exhibiting the high safety and stability (Fig. 4h) [95].

The above two 3D ceramic frameworks can be obtained by using cellulose-based templates, which eliminates the agglomeration issue and

realizes the continuous ion transport. However, these cellulose-derived ceramic frameworks show incomplete structure because of the limited metal ion adsorption sites in cellulose-based templates. According to this, Fu and coworker [96] used silk textile as the template to fabricate a 3D LLZO framework for CPEs. Silk textile is a kind of material rich in multiple functional groups which can adsorb a large number of metal ions (Fig. 4i). The resultant 3D garnet framework well inherits the morphology and structure of the silk template (Fig. 4j), thereby forming the continuous ion transport channels. After penetration of PEO-based electrolyte, the as-obtained CPE has a high filler content of 70 wt%, which contributes the high ionic conductivity, superior thermal and



electrochemical stability. In a word, the template method is a promising approach to fabricate 3D frameworks with favorable structures. In addition, the template method is promising for large-scale manufacture because of the facile and simple preparation process.

The abovementioned works demonstrate that ceramic fiber 3D frameworks can not only provide continuous and long-range ion transport pathways, but also avoid the filler agglomeration in the polymer matrix, which contributes to the highly improved ionic conductivity. However, the brittleness of the ceramic fiber 3D frameworks makes them mechanically too fragile to maintain structure stability during polymer impregnation process and battery fabrication process. Therefore, it is significant to develop new design principles for ceramic fiber 3D frameworks with all-round properties in high ionic conductivity, superior mechanical strength and excellent structure flexibility.

#### 4.1.2. Composite fiber 3D frameworks

Recently, some composite 3D frameworks have been successfully designed and constructed for CSEs to realize both high ionic conductivity and mechanical strength, which will be discussed in detail as follows. Self-assembly strategy has been proved a facile and effective approach to construct the composite 3D frameworks featuring with continuous ion transport channels and desired mechanical robustness. For example, Mai group [97] designed and constructed a hierarchically self-assembled MOF network to provide continuous ion transport and mechanical support for CPEs (Fig. 5a). Through the surface-etching strategy, oriented self-assembly of MOF nanocrystals along the polyimide fibers can be realized. After absorbing the Li-conducting ionic liquid, rapid  $\text{Li}^+$  transport is achieved within the 3D hierarchically self-assembled MOF network. The continuous linear  $\text{Li}^+$  channels are formed

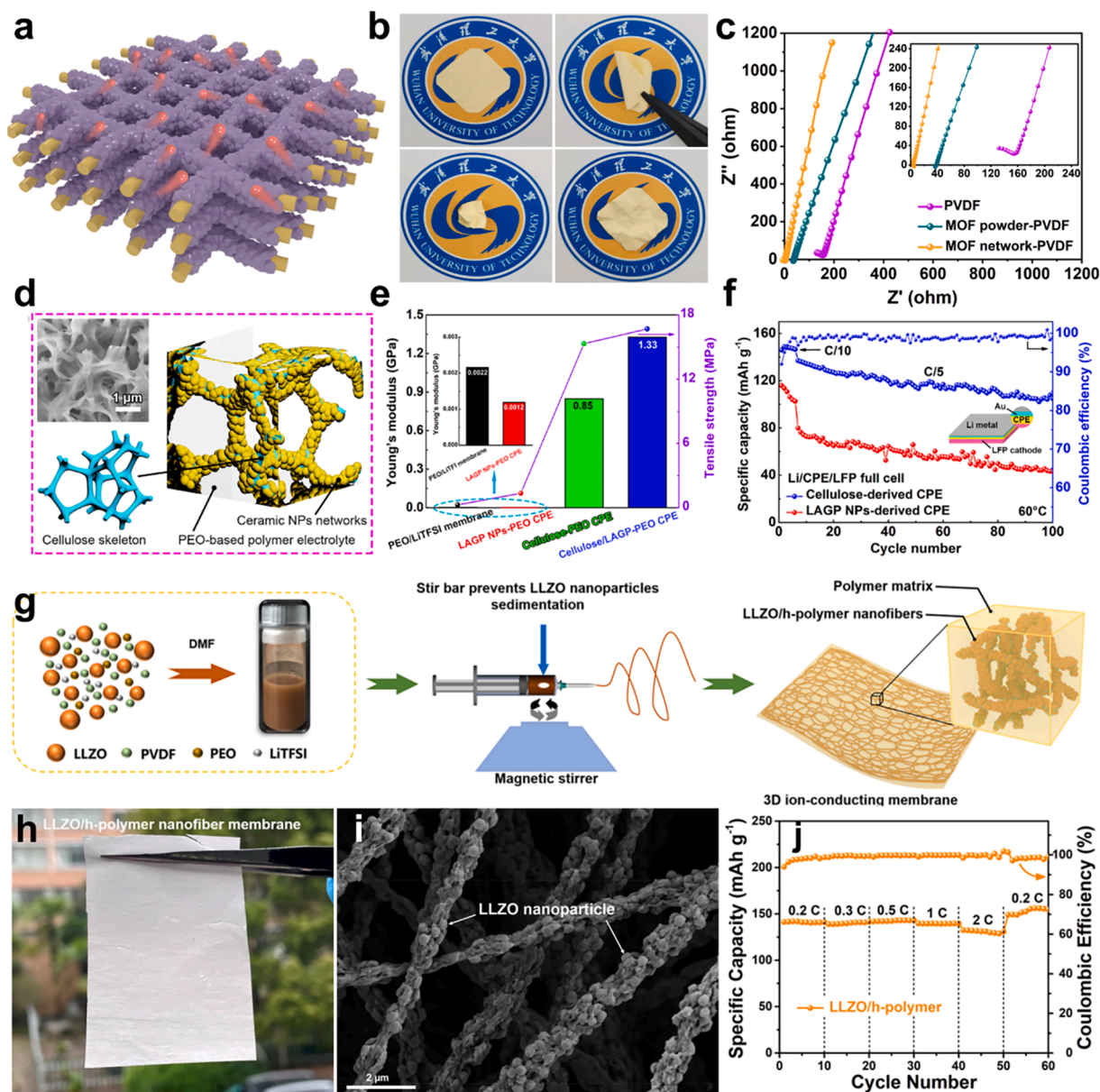


**Fig. 5.** Design of composite fiber 3D frameworks and their application in CPEs for LMBs. (a) Schematic illustration of the hierarchically self-assembled MOF 3D ion conductor. (b) Flexibility test of the self-assembled MOF network. (c) EIS plots of the CPE with 3D MOF network and the counterparts. Reprinted with permission. [97] Copyright 2022, Wiley-VCH. (d) Schematic illustration of the CPE with the 3D cellulose/ceramic network. (e) Young's modulus and tensile strength of CPE with 3D cellulose/ceramic network and other electrolytes. (f) Cycling performance of the solid-state batteries using CPEs with 3D cellulose/ceramic network and ceramic nanoparticles. Reprinted with permission. [100] Copyright 2020, American Chemical Society. (g) Preparation of the CPE with LLZO loaded polymeric nanofiber network. (h) Photographs of the flexible LLZO loaded polymeric nanofiber membrane. (i) SEM image of the LLZO loaded polymeric nanofiber network. (j) Battery performance of the CPE with LLZO loaded polymeric nanofiber network. Reprinted with permission. [101] Copyright 2021, American Chemical Society.

along one-dimensional polyimide fiber direction at the micrometer scale, and the continuous  $\text{Li}^+$  transport in the bulk of resultant solid electrolytes can be obtained based on the 3D structure with interconnected one-dimensional MOF fibers. At the same time, the nanometer-level pores of MOF enable the selective confinement of larger anions for rapid  $\text{Li}^+$  transport. In addition to the high ionic conductivity, the 3D hierarchically self-assembled MOF network also shows high mechanical strength and great flexibility (Fig. 5b), because of the strong banding between MOF and the robust polyimide skeleton. After introduction of the PVDF-based polymer electrolyte, the resulting CPE shows a high ionic conductivity at room temperature and a high mechanical strength (Fig. 5c). Besides, the assembled solid-state  $\text{LiFePO}_4/\text{Li}$  batteries display a great cycling stability. Additionally, another 3D hierarchical MOF network based on two-dimensional  $\text{Cu}(\text{BDC})$  MOF has been developed for high-performance solid electrolytes through the same self-assembly method. The layered MOF can provide one dimensional  $\text{Li}^+$  transport pathways by anchoring anions for free  $\text{Li}^+$ . Furthermore, the 3D hierarchical MOF network enables the 3D continuous  $\text{Li}^+$  transport along the polymer/MOF interface. The nonwoven fabric substrate provides the mechanical support of the 3D hierarchical MOF network and thus endows the 3D framework with great flexibility, which overcome the brittleness issue of MOF materials. As a result, the resulting MOF-network-reinforced composite polymer electrolyte can deliver a desired ionic conductivity and a high  $\text{Li}^+$  transference number, as well as high battery performance with high-voltage  $\text{Li}(\text{Ni}_{0.8}\text{Co}_{0.1}\text{Mn}_{0.1})\text{O}_2$  (NCM811) cathode [98]. Above works confirm the great potential of MOF-based materials for solid-state batteries, which is in accordance with previous reports [99].

In addition to the in-situ growth of MOF materials, the self-assembly strategy can also be used to fabricate 3D ceramic network with both high ionic conductivity and sufficient mechanical strength. For example, a 3D cellulose/ceramic network has been prepared based on natural cellulose fibers and ceramic fillers for CPEs (Fig. 5d). The natural cellulose fibers are characteristic of excellent chemical and thermal stability coupled with desired mechanical strength, which is an ideal candidate as reinforcing skeleton for the 3D ceramic network. With the assistance of vacuum filtration, the ceramic fillers can be self-assembled along the cellulose fibers to form the 3D ceramic network, which can provide 3D continuous  $\text{Li}^+$  transport pathways for high ionic conductivity. Because of the cellulose fiber skeleton, the 3D ceramic network can maintain structure stability during polymer impregnation and battery fabrication process, which contributes to the high mechanical strength of the final CPE and superior battery performance (Fig. 5e,f) [100].

Although the hierarchical MOF networks and the 3D cellulose/ceramic network are fabricated by the self-assembly method, there are some differences between the two works. Specifically, the hierarchical MOF network are constructed by in situ growth of MOF nanocrystals on the surface of supporting substrates, in which the MOF nanocrystals are tightly immobilized on the surface of supporting substrate by chemical bands. While in the fabrication process of the 3D cellulose/ceramic network, the ceramic nanoparticles are directly introduced into the cellulose skeleton with the assistance of vacuum filtration, in which the cellulose skeleton provides spatial guidance for ceramic fillers to be self-assembled along the cellulose fibers and to form the 3D ceramic network.

Besides, a modified electrospinning approach has been developed to fabricate 3D ceramic network for continuous and fast ion conduction and strong robustness. Fu and coworkers [101] constructed a novel 3D ion-conducting nanofiber network composed of LLZO nanoparticles and ion-conducting polymer as binder by a modified electrospinning method (Fig. 5g). In order to realize great flexibility and high ionic conductivity, the ion-conducting binder consisting of PVDF, PEO and lithium salt is explored to spin together with ceramic nanoparticles to form the 3D LLZO nanofiber network. The introduction of PEO reduces the crystallinity of PVDF and promotes  $\text{Li}^+$  transport. In the electrospinning process, the precursor solution has to be stirred constantly to prevent the

LLZO nanoparticles from sedimentating, which is critical to form the highly loaded LLZO nanofibers (Fig. 5i). The resultant 3D LLZO nanofiber network membrane is light and thin while featuring excellent flexibility and mechanical robustness (Fig. 5h). As a result, the assembled solid-state battery using the CPE with the 3D LLZO nanofiber network can display great rate performance and cycling stability (Fig. 5j).

In sum, design and construction of composite 3D frameworks is a promising strategy to obtain desired 3D frameworks with integrated properties in high ionic conductivity, superior mechanical strength and excellent structure flexibility. In order to overcome the brittle issue of the ceramic 3D networks, some effective methods are developed. One is to introduce mechanically robust materials as skeletons for composite 3D frameworks featuring with continuous ion transport channels and desired mechanical robustness. For example, the mechanically robust cellulose network has been used to construct a 3D cellulose/ceramic network for high mechanical strength. In addition, introducing ion-conducting organic polymer as binder into the 3D ceramic frameworks is another effective method. For instance, a novel 3D ion-conducting nanofiber network composed of LLZO nanoparticles and the ion-conducting binder consisting of PVDF, PEO and lithium salt has been designed and fabricated. Accordingly, exploitation of composite 3D frameworks can combine the advantages of different materials, which holds great promise for high-performance CPEs with high ionic conductivity and mechanical strength.

#### 4.2. Vertically aligned 3D frameworks

Vertically aligned 3D frameworks with low tortuosity for CPEs have attracted increasing attention in recent years. Compared with randomly distributed nanoparticles, vertically aligned 3D frameworks can provide shorter ion transport pathways and mechanical support due to their vertically oriented channels and highly ordered structure (Fig. 6a). In 2017, Yang group [36] used a facile ice template method to prepare CPEs with a 3D vertically aligned and interconnected LATP skeleton and PEO-based polymer matrix. They first casted the LATP particle suspension onto the substrate, then applied freeze at the bottom of the substrate, using the temperature gradient to make the particles form vertically aligned structure (Fig. 6b). The flexible CPEs can be obtained by filling the PEO-based polymer matrix into the porous and vertical LATP skeleton which can not only provide short and continuous  $\text{Li}^+$  transfer channels, but also improve the comprehensive performance such as mechanical strength. As shown in Fig. 6c, the as-obtained CPE with the 3D vertically aligned LATP skeleton displays a higher ionic conductivity compared with that with randomly distributed LATP fillers and pure polymer electrolyte. In addition, polyethylene glycol (PEG) was applied in this work to improve the interface contact with electrodes and ionic conductivity. The thermal stability of the composite solid-state electrolyte was also tested, and the results show the increased decomposition temperature with the assistance of the vertical LATP skeleton. After the heating test, the electrolyte with vertically aligned LATP skeleton does not appear obvious curl and other changes compared with pure PEO-PEG electrolyte, which paves the way for the battery operation at high temperature. At the same time, tensile test results indicate that the Young's modulus of the CPEs can be highly increased by incorporating the 3D vertically aligned LATP skeleton. After that, the same group developed another 3D vertically aligned LAGP framework applied in PEO-based electrolyte. The ice-templated LATP skeleton shows a porous and vertical structure with pore sizes between 10 and 20  $\mu\text{m}$  (Fig. 6d). The rational vertically aligned LATP skeleton enables the activation energy of the as-obtained CPE closed to that of the pure LAGP solid electrolyte, which implies that lithium ions mainly transport by LAGP phase, thus delivering a high ionic conductivity (Fig. 6e). Moreover, the resultant composite electrolyte possesses good flexibility with a high ionic conductivity retention after 200 bends. For lithium/lithium cycling test, cells with the LATP-skeleton-reinforced electrolyte work

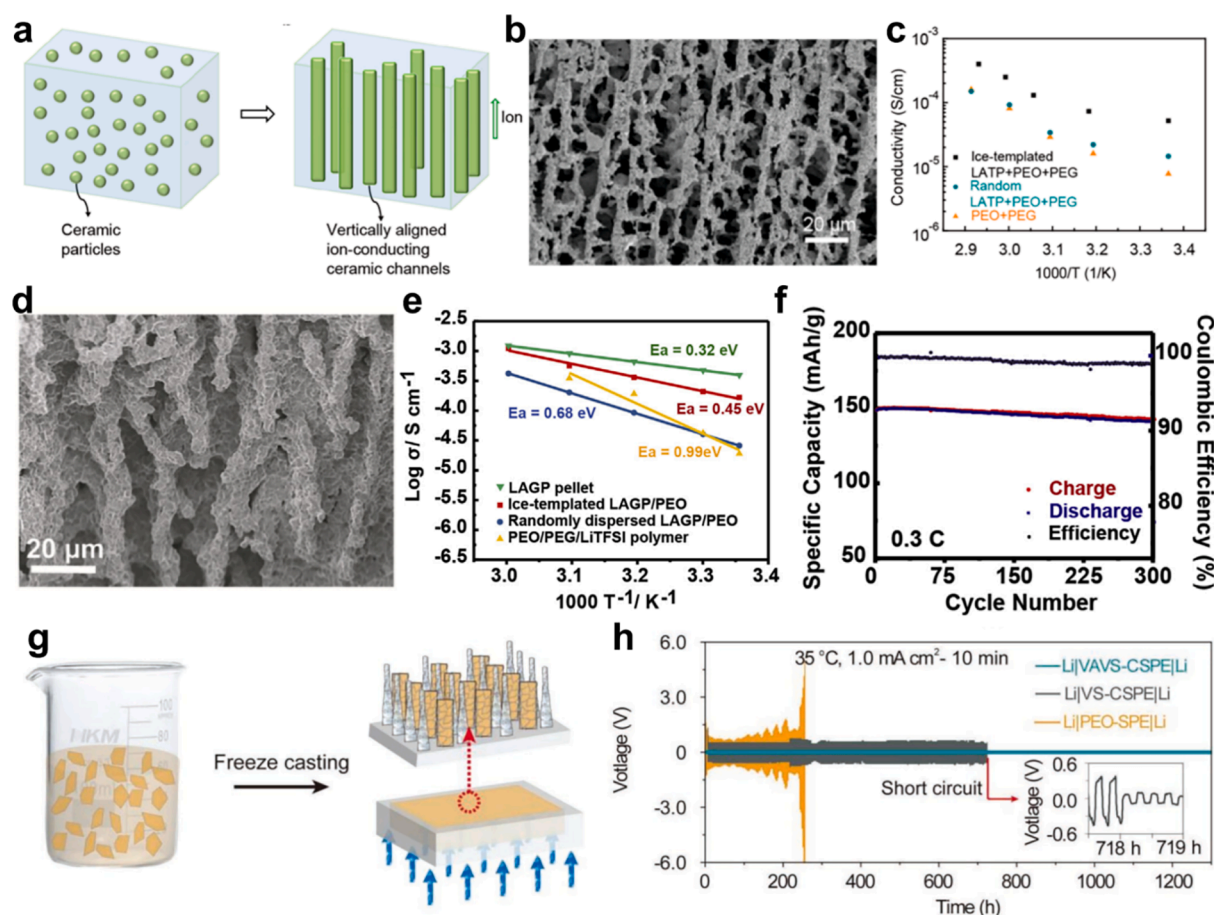


**Fig. 6.** Vertically aligned 3D Frameworks derived from ice-template process and their application in CPEs for LMBs. (a) Schematic illustration of vertically aligned ceramic channels for promoting ion transport. (b) SEM image of the LATP structure with vertically aligned channels. (c) Ionic conductivities of the CPE with vertically aligned LATP skeleton and other electrolytes at various temperatures. Reprinted with permission.[36] Copyright 2017, American Chemical Society. (d) SEM image of the LAGP framework with vertically aligned channels. (e) Arrhenius plots of the vertically aligned LAGP/PEO, randomly dispersed LAGP/PEO, LAGP pellet and polymer electrolytes. (f) Cycling performance of the CPE with vertically aligned LAGP framework. Reprinted with permission.[37] Copyright 2019, Elsevier. (g) Fabrication of vertically aligned vS framework by an ice template method. (h) Comparison of cycling performance of Li symmetric cells with different types of electrolytes. Reprinted with permission.[102] Copyright 2019, Wiley-VCH.

stably with small polarization voltage at different current densities. In addition, the LiFePO<sub>4</sub>-based full battery presents an excellent cycling stability (Fig. 6f) [37]. The ice template method has also been developed by other research groups, for example, Luo group [102] fabricated the 3D vertically aligned framework using 2D vermiculite sheets (VAVS) as starting material for PEO-based solid electrolyte with enhanced ionic conductivity and Li<sup>+</sup> transference number (Fig. 6g). There are abundant and continuous channels in the 2D VAVS, which provides unobstructed and shorter pathways for Li<sup>+</sup> transport. Besides, benefiting from the surface characteristics of the 2D VAVS, Li salts dissociation can be enhanced. Consequently, the as-obtained CPEs can present a high ionic conductivity and a high Li<sup>+</sup> transference number. Another advantage is the remarkable mechanical properties of the as-obtained CPE derived from the 3D vertically aligned VAVS skeleton, which plays an important role to suppress dendrite growth. As a result, the symmetrical metal lithium battery runs over 1300 cycles stably (Fig. 6h). These results indicate that the ice template method is an effective strategy to fabricate 3D vertically aligned structures for high-performance solid electrolytes.

Ice-template method is a simple and effective method for vertically aligned 3D frameworks using ice as the template, which is an environmentally friendly and low-cost approach. And vertically aligned 3D frameworks with low tortuosity can provide shorter and fast ion transport pathways because of the vertically oriented channels and highly ordered structure. But the wide application of the ice-template method for constructing 3D frameworks with vertically aligned structure has

been largely limited. This is because many commonly used inorganic ceramic conductors are unstable in water. In addition, accurate control of the structures is significant and remains challenging due to the fast crystallization process of water. Thus, some modifications and improvements for the ice-template method are required.

Apart from the ice template method, the vertically aligned 3D frameworks can be also obtained from other templates with vertical structure. For instance, Hu group [39] developed a vertically aligned garnet skeleton by using wood as a template. Inspired by the vertical porous structure of the wood, they compressed the original wood with pore size between 10 and 50 μm into the one whose major channels present crack-shaped gaps and some are connected (Fig. 7a). After that they poured the LLZO precursor into the microchannels of the compressed wood, and then annealed the LLZO precursor to form a vertically aligned garnet structure. The well-aligned structure of the natural wood can be well inherited in the final LLZO network (Fig. 7b,c). The 3D garnet skeleton with low tortuosity can provide vertical and continuous Li<sup>+</sup> conduction pathways, which considerably enhances the ionic conductivity of the resultant CPE (Fig. 7d,e). Moreover, the Li/Li cells were assembled, and could work stably without obvious polarization voltage (Fig. 7f,g).

In addition to template method, materials with vertically aligned microchannels can be directly used as 3D frameworks to fabricate high-performance CPEs. Recently, Cui group [103] successfully fabricated a safe, ultrathin and lightweight polymer-polymer electrolyte by

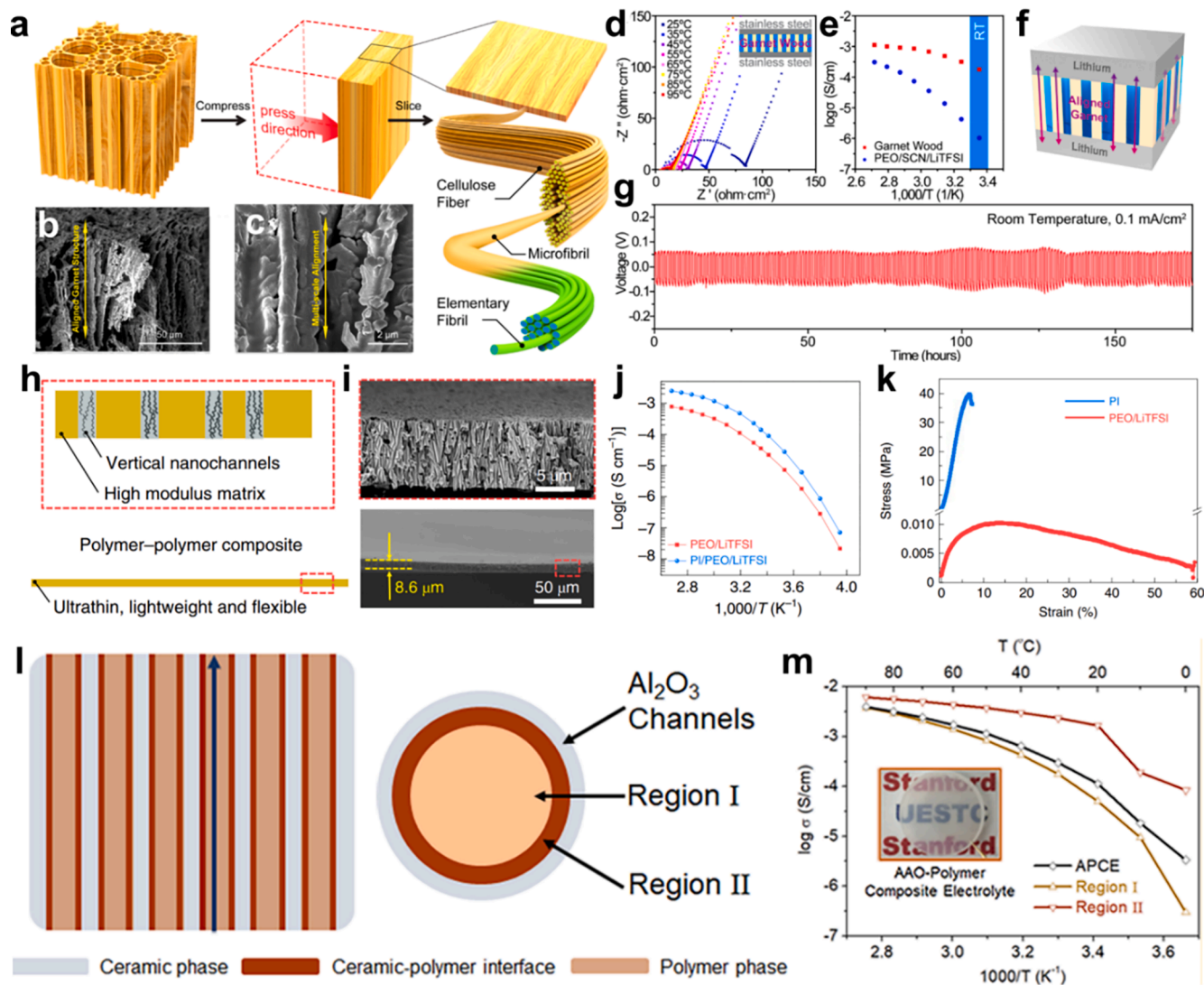


**Fig. 7.** Vertically aligned 3D Frameworks and their application in CPEs for LMBs. (a) Preparation process of the wood template. (b, c) Cross-sectional SEM images of the garnet framework templated by wood. (d) EIS plots of the garnet-wood CPE at various temperatures. (e) Comparison of ionic conductivities of the garnet-wood and PEO-based polymer electrolyte. (f) Schematic of the symmetric Li cell with garnet-wood CPE. (g) Electrochemical stability of Li symmetric cell with garnet-wood CPE. Reprinted with permission.[39] Copyright 2019, American Chemical Society. (h) Design of the polymer-polymer CPE using the ultrathin porous polyimide host. (i) Cross-sectional SEM images of the ultrathin porous polyimide host. (j) Comparison of ionic conductivities of the polyimide-reinforced and PEO-based polymer electrolytes. (k) Stress-strain curve of the ultrathin porous polyimide film and PEO-based polymer electrolytes. Reprinted with permission.[103] Copyright 2019, Springer Nature. (l) Schematics of ceramic-polymer interface in AAO-reinforced CPE. (m) Calculated ionic conductivities of region I and region II in AAO-reinforced CPE and measured ionic conductivities of AAO-reinforced CPE. Reprinted with permission.[84] Copyright 2018, American Chemical Society.

embedding polymer electrolyte into the vertical nanochannels of the polyimide (PI) host (Fig. 7h). The ultrathin and porous PI matrix possesses vertically aligned nanochannels and a thickness of 8.6  $\mu\text{m}$ , which can be seen in Fig. 7i. Because of the vertically aligned nanochannels, this polymer-polymer composite electrolyte delivers a highly enhanced ionic conductivity, and the simulation results reveal that  $\text{Li}^+$  tend to transport along the vertical alignment direction, which may explain the improved ionic conductivity of PEO-based polymer electrolyte in the aligned channels. Besides, the nanoconfinement effect of PEO-based polymer electrolyte in the nanochannels may facilitate the fast Li ions diffusion (Fig. 7j). In addition, the PI skeleton is nonflammable and mechanically robust (Fig. 7k), and the Li-Li cells are stable over 1000 h without short circuit. In the abuse test, the as-assembled pouch cell can withstand harsh conditions such as bending, twisting, cutting and nail perforation, which indicates the high safety and flexibility of the polymer-polymer composite electrolyte. Meanwhile, the same group explored  $\text{AlF}_3$ -modified AAO with vertically aligned structure as a 3D

framework for polymer electrolytes. The porous AAO can provide vertically aligned channels with an average diameter of 200 nm, which can provide fast and continuous ionic conduction pathways along the interface between the vertically aligned channels of AAO and PEO electrolyte (Fig. 7l). The Lewis acid-base interaction between the  $\text{AlF}_3$ -modified AAO and PEO chains results in the superior conductivity (Fig. 7m). Experimental results show that  $\text{Li}^+$  can transport rapidly along the vertically aligned interface, which is likely to release super ion conduction. Moreover, the smart design of this composite electrolyte enables the Li-Li battery with superior cycle stability without Li dendrite penetration [84]. Based on aforementioned great works, the application of vertically aligned 3D frameworks provides a new idea for the development of high-performance solid electrolytes.

In summary, using materials with vertically aligned microchannels as 3D frameworks is a simple and direct method to modify the polymer electrolytes. The polymer electrolytes in the vertically aligned channels deliver a higher ionic conductivity, suggesting that  $\text{Li}^+$  tend to transport

along the vertical alignment direction. But the used 3D frameworks with vertically aligned channels are inert materials, which fail to conduct Li ions themselves. Besides, the vertically aligned pores inside the 3D frameworks are limited. So, the fast ion conduction interfaces are deficient, which leads to the limited ionic conductivity improvement. Therefore, development of highly conductive materials with vertically aligned microchannels as 3D frameworks or increase of the fast ion

conduction interfaces are future direction.

### 4.3. Porous aerogel/hydrogel-derived 3D frameworks

#### 4.3.1. Porous aerogel-derived 3D frameworks

To promote the  $\text{Li}^+$  transport, solid polymer electrolytes are generally applied at increased temperature for facilitating the segmental

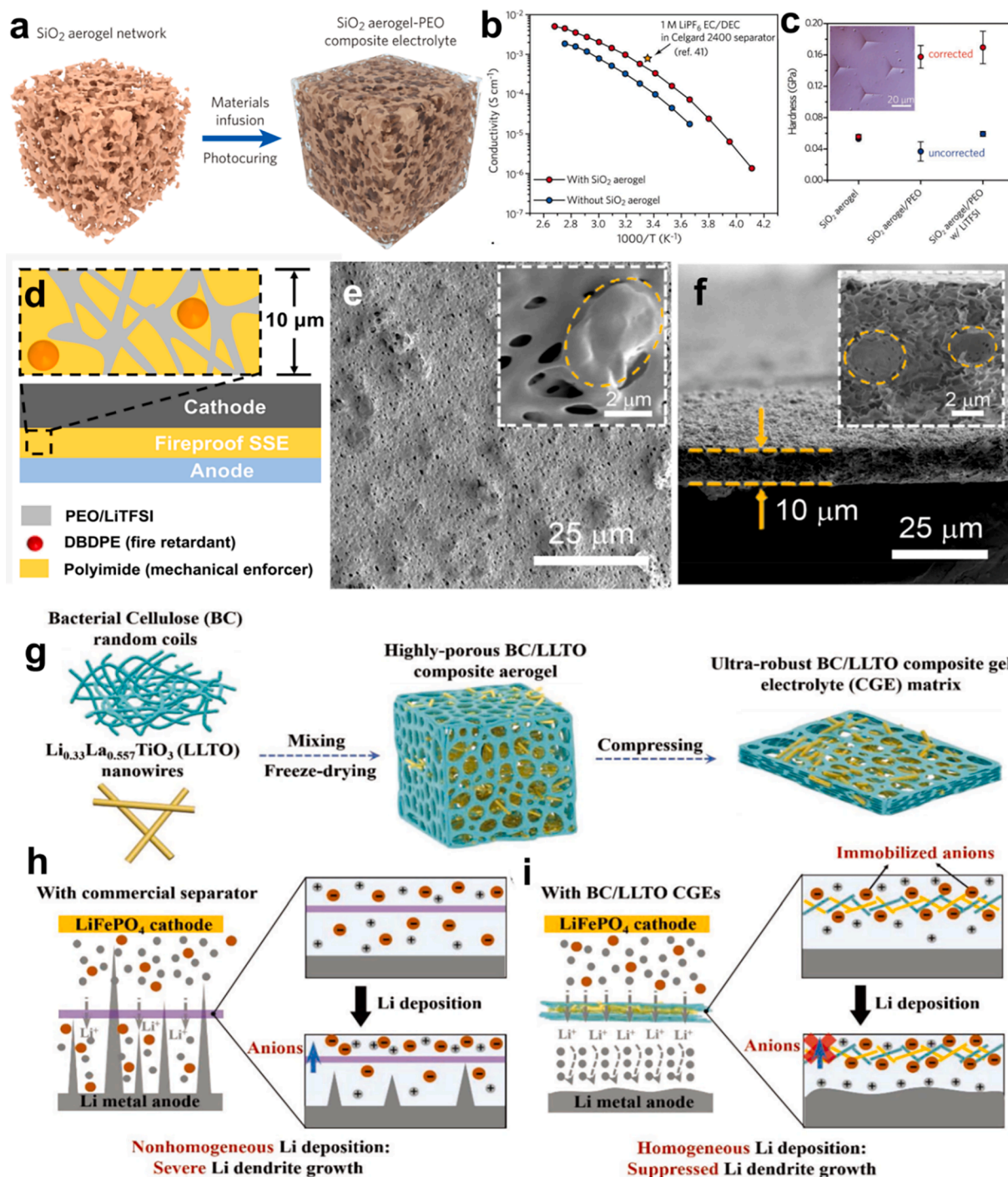


**Fig. 8.** Design of porous aerogel-derived 3D frameworks and their application in CPEs for LMBs. (a) Schematic illustration of the CPE based on the 3D  $\text{SiO}_2$  aerogel skeleton. (b) Comparison of ionic conductivities of the electrolytes with and without 3D  $\text{SiO}_2$  aerogel skeleton. (c) Hardness of the  $\text{SiO}_2$  aerogel,  $\text{SiO}_2$  aerogel/PEO composite, and  $\text{SiO}_2$  aerogel/PEO/LiTFSI CPE. Reprinted with permission.[104] Copyright 2018, Wiley-VCH. (d) Design principle of the fireproof and ultrathin CPE based on the porous robust 3D polyimide skeleton. (e) SEM image of the surface of the porous polyimide skeleton. (f) Cross-section SEM image of the porous polyimide skeleton. Reprinted with permission.[105] Copyright 2020, American Chemical Society (g) Preparation process of the porous BC/LLTO aerogel. Schematic illustration of the Li deposition of (h) Commercial separators and (i) The BC/LLTO composite gel electrolyte. Reprinted with permission.[106] Copyright 2019, Wiley-VCH.

motion of the polymer, which will contribute to fast ion conduction. However, the elevated temperatures deteriorate the mechanical strength of polymer electrolytes and compromise the safety of batteries. In order to solve this issue, 3D aerogel frameworks have been designed and constructed for solid polymer electrolytes. The 3D aerogel frameworks commonly exhibit high elastic modulus, high porosity and large internal surface area. Incorporation of the 3D aerogel frameworks can improve the mechanical strength, thus helps to effectively inhibit the Li dendrite growth. The high porosity further facilitates to accommodate high-content polymer electrolytes, which enables sufficient Li ion conduction. Meanwhile, the well-distributed fillers within the 3D aerogel frameworks promote Lewis acid-base interactions, thereby enabling high dissociation of lithium salts and boosting the ionic conductivity. For example, a mechanically strong CPE was developed by compositing a 3D SiO<sub>2</sub> aerogel skeleton and conductive PEO matrix as shown in Fig. 8a. The 3D SiO<sub>2</sub> aerogel framework exhibits a well-organized and highly porous structure with a large internal surface area, which can provide large and continuous interfaces for Li ions to transport within a long distance based on Lewis acid-base effect, hence contributing to the highly improved ionic conductivity (Fig. 8b). Another benefit of the 3D SiO<sub>2</sub> aerogel framework is that it can act as a robust backbone to reinforce the PEO electrolytes, resulting in a higher elastic modulus and a considerably improved hardness (Fig. 8c). Owing to this, the resultant composite electrolyte can effectively suppress lithium dendrite growth, facilitating a stable long-term cycling life. As a result of the 3D SiO<sub>2</sub> aerogel skeleton, LiFePO<sub>4</sub>/Li full cells function well with high rate capability and excellent cyclic stability [104]. Afterwards, the same research group developed a porous and robust polyimide (PI) skeleton for ultrathin and non-flammable CPE. The flame retardant (decabromodiphenyl ethane, DBDPE) was introduced into the polyimide skeleton, which can not only provide strong mechanical strength to inhibit lithium dendrite growth, but also avoid fire risks (Fig. 8d). The PI/DBDPE skeleton presents a porous structure with a pore size about 500 nm, in which the DBDPE particles are uniformly distributed within PI matrix (Fig. 8e,f). Notably, pouch cells assembled with the fireproof electrolyte can function well after being exposed to flame for 24 s, demonstrating the suitability for solid-state LMBs with high safety [105]. To further enhance the ionic conductivity, Zhong and co-workers [106] combine advantages of mechanical strength of bacterial cellulose (BC) and fast ion conduction of LLTO nanowires to design a 3D interconnected porous aerogel skeleton as presented in Fig. 8g. The 3D BC/LLTO aerogel framework displays a hierarchical structure with multi-scale pores for remarkable liquid electrolyte uptake. Because of the 3D BC/LLTO skeleton, the resultant gel electrolyte shows high mechanical strength and high Li-ion transference number. Most intriguingly, the brilliant composite framework can facilitate uniform ion deposition and thus suppress dendrite formation (Fig. 8i), which enables the stable long-term Li-Li cycling more than 1200 h without failure. According to the above-mentioned results, the stiff 3D aerogel frameworks really play a vital role in design and fabrication of CPEs with improved comprehensive properties.

These three representative works indicate the possibility of the 3D aerogel frameworks, which can improve the mechanical strength of CPEs to effectively inhibit the Li dendrite growth. Furthermore, the porous 3D aerogel frameworks with Lewis acid sites can enable high dissociation of lithium salts and boost the ionic conductivity. However, the construction of 3D aerogel frameworks still faces some challenges. For example, the 3D SiO<sub>2</sub> aerogel framework suffers from the brittleness issue. And the porous polyimide skeleton shows great flexibility, but the polyimide framework fails to conduct Li ions itself and provide Lewis acid sites or oxygen vacancies to promote ion transport. The composite 3D BC/LLTO aerogel framework can combine the mechanical advantage of BC and high ionic conductivity of the LLTO nanowires, which holds great promise for CPEs.

#### 4.3.2. Porous hydrogel-derived 3D frameworks

Introducing inorganic fillers in CPEs can enhance their mechanical property and electrochemical performance. However, the content of the ceramic fillers is severely restricted owing to the agglomeration effect, resulting in limited enhancement of ionic conductivity. 3D porous hydrogel is a kind of material featuring with porous and tunable structures, simple preparation process and easy large-scale manufacture. Recently, there are some successful applications of the ceramic hydrogel-derived 3D frameworks in CPEs, which can achieve higher ionic conductivity and desired electrochemical stability. For instance, a 3D hydrogel-derived LLTO structure was developed by Yu group [55] for continuous ion transport. The hydrogel-derived LLTO framework exhibits a well-percolated and porous structure (Fig. 9a), and the structure can be well preserved after introduction of PEO-based electrolyte into the LLTO framework (Fig. 9b), which could provide continuous Li<sup>+</sup> transport pathways for high ionic conductivity (Fig. 9c). After that, they designed another 3D hydrogel-derived framework by using LLZO ion conductor, which could be obtained by gelation and heat treatment of the LLZO precursor. The final 3D hydrogel-derived LLZO skeleton presents an interconnected and highly porous structure (Fig. 9d). Meanwhile, the as-prepared CPE can maintain excellent flexibility regardless of bending or winding, showing desired mechanical properties (Fig. 9e). Even after heat treatment, this electrolyte can still maintain a high integrity (Fig. 9f), and effectively avoid the risk of thermal runaway, which can be attributed to the introduction of the 3D hydrogel-derived LLZO skeleton. And the TG test indicates the lower crystallinity of PEO chains and high content of LLZO ion conductor due to the 3D hydrogel-derived LLZO skeleton (Fig. 9g), which results in improved Li<sup>+</sup> conductivity [56].

Besides, Guo's group [107] have reported a well-organized porous 3D garnet skeleton with a continuous channel structure (~20 μm) by exploiting polyurethane foam as a template, which can provide continuous Li ion conduction paths and heighten the mechanical strength of the composite electrolyte. Due to this, the 3D garnet skeleton reinforced electrolyte displays an ionic conductivity of  $1.2 \times 10^{-4}$  S cm<sup>-1</sup> at room temperature, much higher than that of one with randomly dispersed LLZO particles. Similarly, a 3D porous LLZTO backbone was fabricated by using cellulose and polyester (CP) textile as a template. After calcination process, the obtained LLZTO backbone shows a porous morphology with average-grain size of ~5 μm, offering interconnected Li-conducting channels and resulting in an improved conductivity of  $2.61 \times 10^{-4}$  S cm<sup>-1</sup> at room temperature. Consequently, the resultant CPE exhibits a high transference number of 0.71 and desirable thermal stability. Furthermore, the low-cost gel-casting method employed in this work can have a wide application in other composite electrolytes to design and fabricate rational ceramic frameworks with unique structures [108].

In sum, the 3D interconnected hydrogel-derived frameworks have shown great potential in solid-state LMBs owing to their fast ion-conducting ability and easy preparation process. Unfortunately, the 3D hydrogel-derived frameworks still face the same challenge in flexibility due to the brittle feature of inorganic ceramic materials. Besides, how to accurately control the porous structures remains difficult. And the extension of more materials for 3D hydrogel-derived frameworks is worth exploring.

#### 4.4. Brick-like 3D frameworks

Inorganic solid electrolytes commonly display desirable ionic conductivity ( $10^{-4} \sim 10^{-3}$  S cm<sup>-1</sup>), and good electrochemical stability. Unfortunately, the brittleness of these ceramic electrolytes makes them mechanically fragile, which limits their practical application. As we all know, natural nacre is one of the most promising biomaterials with a special "brick-and-mortar" structure composed of brittle CaCO<sub>3</sub> platelets and soft protein polymer layers, which combines both ultrahigh mechanical strength and excellent toughness (Fig. 10a) [109]. Inspired by

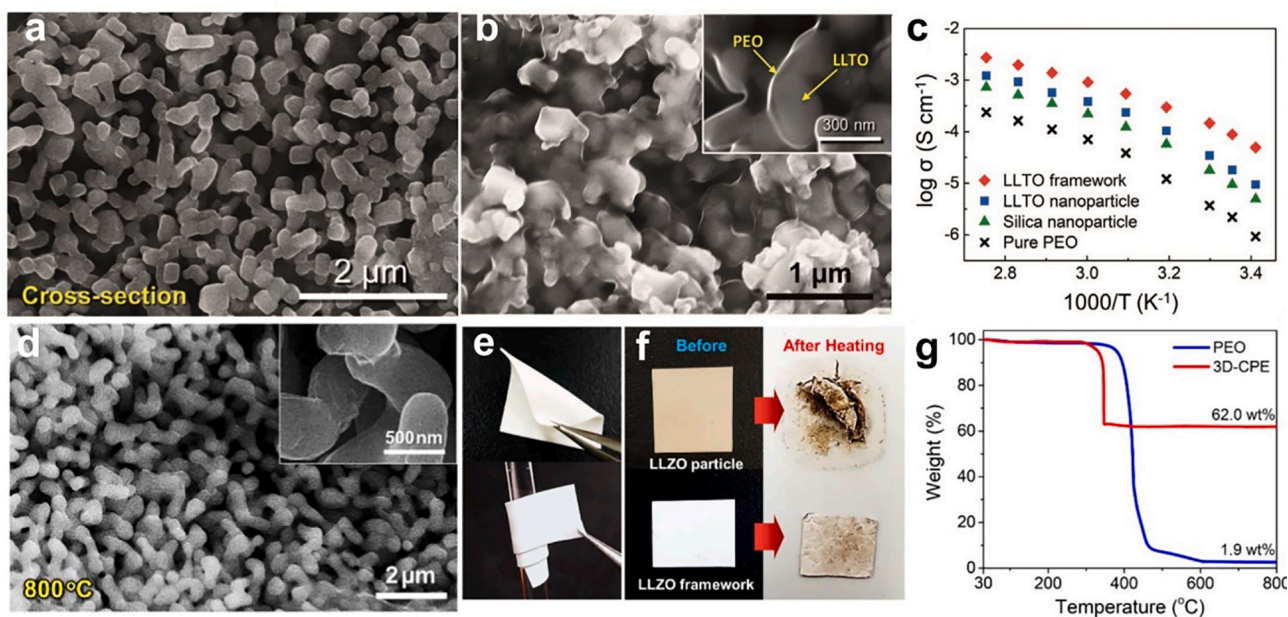


**Fig. 9.** Design of porous hydrogel-derived 3D frameworks and their application in CPEs for LMBs. (a) Cross-section SEM image of the LLTO framework. (b) Cross-section SEM image of the CPE with LLTO framework. (c) Comparison of ionic conductivities of the CPE with LLTO framework and other electrolytes. Reprinted with permission. [55] Copyright 2018, Wiley-VCH. (d) Cross-section SEM image of the LLZO framework. (e) Flexibility test of the CPE with LLZO framework. (f) Heating test of the CPE with LLZO particles and LLZO framework. (g) TG test of the CPE with LLZO framework and PEO-based electrolyte. Reprinted with permission. [56] Copyright 2018, Elsevier.

this “brick-and-mortar” structure, ceramic electrolytes as the “bricks” glued by elastic polymer matrix as the “grout” are promising to realize the coexistence between flexibility and mechanical robustness of the CPEs. For this reason, a facile bottom-up method was developed to design a composite solid electrolyte with a “brick-and-mortar” layout design, in which LAGP platelets function as the “brick” and polymer matrix as the “mortar”, aiming to address the mechanical strength issue in solid electrolytes (Fig. 10b,c). As a result, the nacre-like ceramic/polymer electrolyte realizes a much higher fracture strain than pure ceramic electrolyte. Besides, a much larger ultimate flexural modulus can be obtained for the nacre-like solid electrolyte compare to pure polymer electrolytes. The improved mechanical strength of the nacre-like electrolyte is also proved by the ball impact tests (Fig. 10d). Most intriguingly, full cells with the nacre-like ceramic/polymer electrolyte can work stably even under a heavy load. In contrast, batteries using pure ceramic electrolytes or pure polymer electrolytes fail to function well in the same condition. Besides, Hu group [43] proposed a similar design strategy for a composite solid electrolyte membrane with the “brick-and-mortar” pattern. Using the 3D printing manufacturing method (Fig. 10e), brick-like LLZO chips are connected well without gaps by using styrene-butadiene copolymer (SBC) as the mortar (Fig. 10f-j). The brick-like LLZO chips can provide fast ion-conducting paths, while the SBC releases the strain caused in preparation process, packaging process, transportation process and application. It is worth noting that fracture mechanics analysis was conducted to design the optimum size of the LLZO chips with diverse membrane thicknesses to form strong bonding between the brick-like LLZO chips and mortar-like polymer. As a result, the resultant composite electrolyte displays an excellent extensibility of 220 % with a final tensile strength of 5.12 MP, which enables the superior flexibility and cycling stability under bending. Using the same 3D printing method, a new type “brick-and-mortar” CPE with 3D bi-continuous ordered ceramic electrolyte and polymer matrix has been constructed as shown in Fig. 10k. This method can precisely control the ratio of polymer to ceramic and realize the 3D bi-continuous ordered ceramic. The CPE used LAGP as the “brick”, and filled empty channels with polymers as “mortar”. To be specific, as shown in Fig. 10k, the first stage is to fabricate the 3D printed polymer-

based template, followed by introduction of LAGP powder into empty channels. After removing the polymer template through sintering process, the 3D bi-continuous ordered LAGP skeleton can be formed. At last, flexible polymers fill the empty channels to obtain the final composite electrolyte with 3D bi-continuous ordered structures. After being tested, the gyroidal composite electrolyte delivers optimal electrochemical properties, like acceptable ionic conductivity of  $1.6 \times 10^{-4}$  S cm<sup>-1</sup> and better cycling stability. It is also worth noting that this electrolyte displays higher mechanical strength in comparison with the pure ceramic electrolyte, which is important for batteries to meet the high safe requirement [44].

Indeed, these works inspire us that composite electrolytes with “brick-and-mortar” structures can not only possess remarkable mechanical performance, but also deliver improved ionic conductivity, which provides a new design principle for future composite solid electrolytes with mechanical robustness. But the polymer materials using as the “mortar” in above works are ionically insulating, which limits the further ionic conductivity enhancement. Therefore, using ionically conductive polymer materials as “mortar” can realize the coexistence between flexibility and mechanical robustness without compromising the ionic conduction of the inorganic ceramic electrolytes. In addition, further optimizing the “brick-and-mortar” structures to effectively utilize the advantages of highly conductive inorganic ceramic electrolytes and elastic polymer deserves more efforts.

In addition to all above discussions, construction of 3D crosslinked networks for polymer electrolytes is also an effective strategy to enable high ionic conductivity and high mechanical strength. Lu et al. developed a ring-opening polymerization method without initiator to fabricate a rigid 3D cross-linked network in gel polymer electrolyte, in which rigid polymer component serves as reinforcing skeleton for mechanical support, and soft polymer component is used to enable rapid Li<sup>+</sup> conduction [110]. Then, a 3D crosslinked network PEO@nano-SiO<sub>2</sub> composite polymer electrolyte was designed to enhance ion conduction and mechanical properties. In this work, nano-sized SiO<sub>2</sub> is used as cross-linking agent to form the cross-linked structure, and simultaneously improves the ion transport and reinforces the whole composite polymer electrolyte [111]. Recently, Liang et al. constructed a novel gel polymer

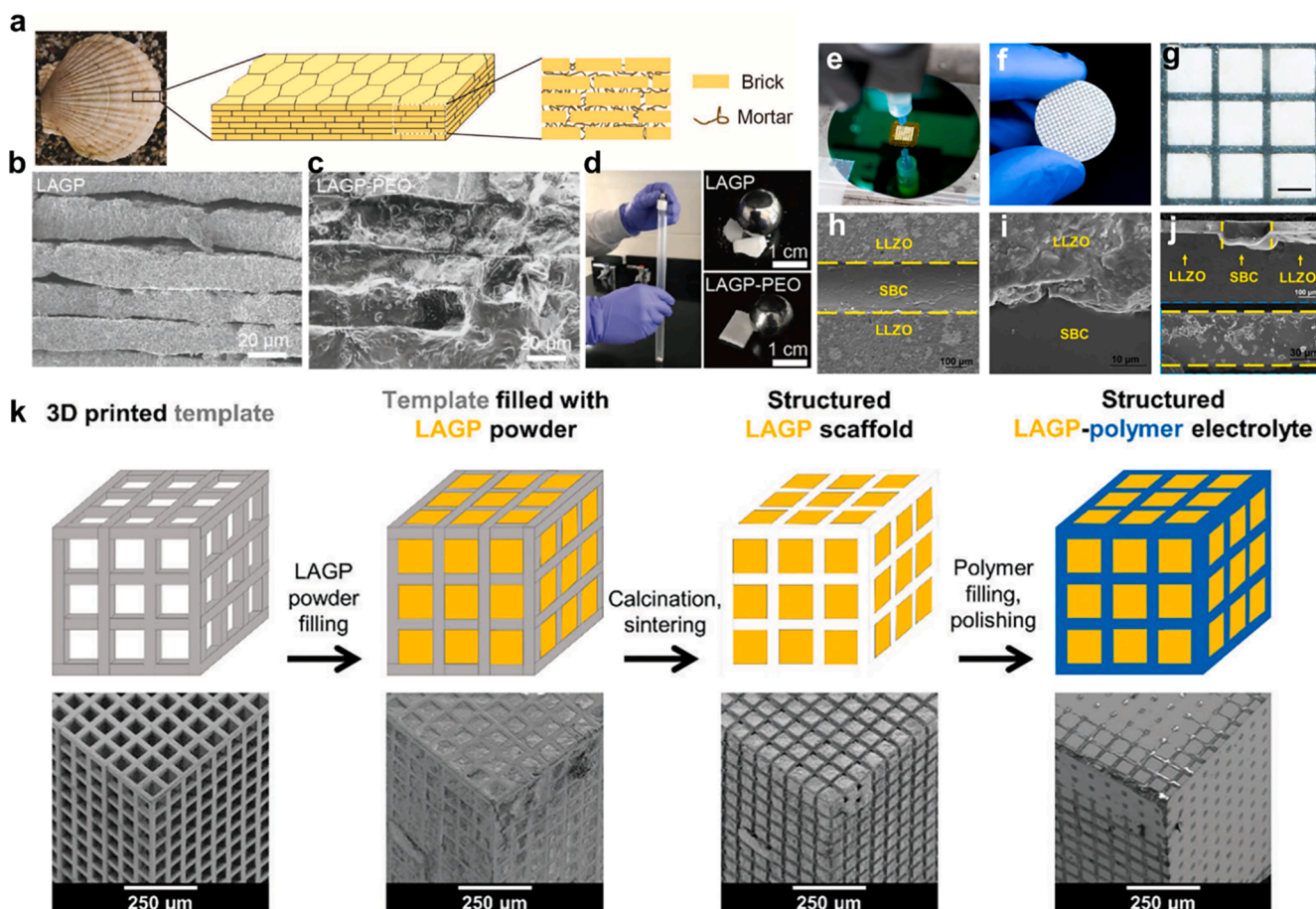


**Fig. 10.** Design of brick-like 3D frameworks and their application in CPEs for LMBs. (a) Schematic illustration of the “brick-and-mortar” structure in nacre. (b) Cross-section SEM image of the layered LAGP tablets. (c) Cross-section SEM image of the “brick-and-mortar” CPE. (d) Impact test of the “brick-and-mortar” CPE and pure LAGP membrane. Reprinted with permission. [109] Copyright 2020, Wiley-VCH. (e) Photograph of the binding process by a 3D printing method. (f, g) Photographs of the CPE with tile-and-grout structure. (h, i) SEM images of the connecting region of the LLZO and the polymer. (j) Cross-section SEM image of the connecting region of the LLZO and the polymer. Reprinted with permission. [43] Copyright 2019, American Chemical Society. (k) Preparation process of the CPE with 3D bi-continuous ordered LAGP skeleton derived from a 3D printed template. Reprinted with permission. [44] Copyright 2018, The Royal Society of Chemistry.

electrolyte with a 3D compact and crosslinked structure via in-situ copolymerization of polymer matrix in liquid electrolytes. Benefiting from the 3D crosslinked network, uniform  $\text{Li}^+$  flux can be achieved, which enables the stable  $\text{Li}^+$  deposition on the lithium anode surface [112]. Besides, Zuo et al. designed a solid polymer electrolyte with a multifunctional 3D crosslinked network with the assistance of thioctic acid, which can make flexible PEGDA polymerize in rigid PVDF-HFP matrix to form the multifunctional 3D crosslinked network. This functional 3D crosslinked network can not only provide continuous  $\text{Li}^+$  transport pathways, but also highly enhance the mechanical strength [113].

## 5. Conclusion and outlook

This review discusses the development of 3D frameworks in composite solid electrolytes for solid-state LMBs. 3D frameworks can be categorized based on structural characteristic and chemical composition, including vertically aligned 3D frameworks, 3D fiber frameworks, porous aerogel-derived 3D frameworks, porous hydrogel-derived 3D frameworks and ordered brick-like 3D frameworks. We discuss, in detail, structure design and synthesis of these 3D frameworks and the ion-conducting mechanisms in the CPEs. Furthermore, according to different types of 3D frameworks, we introduce their applications in CPEs for high-performance solid-state batteries.

Based on our discussion, 3D frameworks in CPEs have remarkably

promoted the comprehensive properties, which makes rapid development of solid lithium-ion batteries. Nonetheless, there are some challenges and future directions from fundamental mechanisms to practical applications as follows.

1. Revelation of the in-depth mechanisms. Multifunctional 3D frameworks have considerably improved the comprehensive properties of CPEs, and a deep understanding of the enhanced properties deserves special focus. For example, ion transport mechanisms and ion diffusion dynamics of the 3D frameworks and the polymer phase should be investigated. In addition, the buried interfaces and the physical/chemical interactions between the 3D frameworks and the polymer matrix should be explored and analyzed. To address above questions, state-of-the-art technologies like in-situ observation approaches or other advanced methods are required. Besides, artificial intelligence and machine learning should be developed for investigating the ion transport mechanisms and ion diffusion dynamics of the CPEs with 3D frameworks. By doing this, it is highly helpful to design and construct advanced CPEs for high-performance solid-state LMBs.
2. Further improvement of the ionic conductivity. Although diverse types of 3D frameworks applied in CPEs have been developed to promote  $\text{Li}^+$  ions transport, the ionic conductivity are commonly below  $10^{-3} \text{ S cm}^{-1}$ , which need to be further enhanced to the necessary value of  $10^{-3} \sim 10^{-2} \text{ S cm}^{-1}$ . In order to address this issue,



the 3D frameworks should meet some requirements: one is that the 3D frameworks display superionic conduction, whose ionic conductivity is on the order of  $\text{mS cm}^{-1}$ . Besides, 3D frameworks with large surface area are benefit of enabling high-content interfacial regions for fast ionic conduction, which is significant for highly improved ionic conductivity of the composite solid electrolytes. In general, material selection will be a hard work, artificial intelligence and machine learning can avoid many time-consuming experiments.

3. A higher  $\text{Li}^+$  transference number. A high  $\text{Li}^+$  transference number plays a critical role in stable battery operation. Insufficient  $\text{Li}^+$  transference number can cause concentration gradient of ions and lead to polarization, which induces the formation of lithium dendrites. To this end, some approaches should be developed for enhancing the  $\text{Li}^+$  transference number of composite polymer electrolytes. One way is to anchor anions to polymer matrix by grafting some functional groups into the polymer chains, which can reduce the mobility of anions and result in a high  $\text{Li}^+$  transference number. Another method is to design and construct 3D frameworks with rich oxygen vacancies or Lewis acid sites to immobilize the anionic ions, which facilitates the Li salts dissociation and hence releases more free Li ions.
4. Mass production of CPEs with 3D frameworks. Solid-state CPEs with 3D frameworks can effectively increase the energy density and achieve high safety by replacing flammable liquid electrolytes. Nevertheless, it is challenging to realize low-cost manufacture of CPEs with 3D frameworks because of the immature technology. In order to realize mass production, it is necessary to modify the preparation process of composite polymer electrolytes with 3D frameworks. For example, new manufacture techniques for thin and flexible composite solid electrolytes with 3D frameworks are desired.

#### Declaration of Competing Interest

The authors declare that they have no known competing financial interests or personal relationships that could have appeared to influence the work reported in this paper.

#### Data availability

No data was used for the research described in the article.

#### Acknowledgements

This work was supported by the National Key Research and Development Program of China (2019YFA0704900), the National Natural Science Foundation of China (51802239), the Key Research and Development Program of Hubei Province (2021BAA070), Foshan Xianhu Laboratory of the Advanced Energy Science and Technology Guangdong Laboratory (XHT2020005), and the Fundamental Research Funds for the Central Universities (2020011GX, 2020IVB057, 2019IVB054, 2019III062JL).

#### References

- [1] A. Manthiram, X.W. Yu, S.F. Wang, Lithium battery chemistries enabled by solid-state electrolytes, *Nat. Rev. Mater.* 2 (4) (2017) 16103.
- [2] J. Janek, W.G. Zeier, A solid future for battery development, *Nat. Energy* 1 (2016) 16143.
- [3] D.C. Lin, Y.Y. Liu, Y. Cui, Reviving the lithium metal anode for high-energy batteries, *Nat. Nanotechnol.* 12 (3) (2017) 194–206.
- [4] X. Meng, K.C. Lau, H. Zhou, S.K. Ghosh, M. Benamara, M. Zou, Molecular layer deposition of crosslinked polymeric lithicone for superior lithium metal anodes, *Energy Mater. Adv.* 2021 (2021) 9786201.
- [5] X.B. Cheng, R. Zhang, C.Z. Zhao, Q. Zhang, Toward safe lithium metal anode in rechargeable batteries: a review, *Chem. Rev.* 117 (15) (2017) 10403–10473.
- [6] J. Xiao, How lithium dendrites form in liquid batteries, *Science* 366 (6464) (2019) 426–427.
- [7] M. Hu, X.L. Pang, Z. Zhou, Recent progress in high-voltage lithium ion batteries, *J. Power Sources* 237 (2013) 229–242.
- [8] L.Z. Fan, H.C. He, C.W. Nan, Tailoring inorganic-polymer composites for the mass production of solid-state batteries, *Nat. Rev. Mater.* 6 (11) (2021) 1003–1019.
- [9] C.P. Yang, Q.S. Wu, W.Q. Xie, X. Zhang, A. Brozena, J. Zheng, M.N. Garaga, B. H. Ko, Y.M. Mao, S.M. He, Y. Gao, P.B. Wang, M. Tyagi, F. Jiao, R. Briber, P. Albertus, C.S. Wang, S. Greenbaum, Y.Y. Hu, A. Isogai, M. Winter, K. Xu, Y. Qi, L.B. Hu, Copper-coordinated cellulose ion conductors for solid-state batteries, *Nature* 598 (7882) (2021) 590–596.
- [10] Y.Y. Sun, Q. Zhang, L. Yan, T.B. Wang, P.Y. Hou, A review of interfaces within solid-state electrolytes: fundamentals, issues and advancements, *Chem. Eng. J.* 437 (2022), 135179.
- [11] Z.H. Gao, H.B. Sun, L. Fu, F.L. Ye, Y. Zhang, W. Luo, Y.H. Huang, Promises, challenges, and recent progress of inorganic solid-state electrolytes for all-solid-state lithium batteries, *Adv. Mater.* 30 (17) (2018) 1705702.
- [12] Y. Meesala, A. Jena, H. Chang, R.S. Liu, Recent advancements in Li-ion conductors for all-solid-state Li-ion batteries, *ACS Energy Lett.* 2 (12) (2017) 2734–2751.
- [13] W.P. Chen, H. Duan, J.L. Shi, Y.M. Qian, J. Wan, X.D. Zhang, H. Sheng, B. Guan, R. Wen, Y.X. Yin, S. Xin, Y.G. Guo, L.J. Wan, Bridging interparticle  $\text{Li}^+$  conduction in a soft ceramic oxide electrolyte, *J. Am. Chem. Soc.* 143 (15) (2021) 5717–5726.
- [14] R.Y. Fang, B.Y. Xu, N.S. Grundish, Y. Xia, Y.T. Li, C.W. Lu, Y.J. Liu, N. Wu, J. B. Goodenough,  $\text{Li}_2\text{S}_6$ -integrated PEO-based polymer electrolytes for all-solid-state lithium-metal batteries, *Angew. Chem. Int. Edit.* 60 (32) (2021) 17701–17706.
- [15] F. Liu, Y. Cheng, X.R. Zuo, R.P. Chen, J.Y. Zhang, L.Q. Mai, L. Xu, Gradient trilayer solid-state electrolyte with excellent interface compatibility for high-voltage lithium batteries, *Chem. Eng. J.* 441 (2022), 136077.
- [16] H. Gao, N.S. Grundish, Y. Zhao, A. Zhou, J.B. Goodenough, Formation of stable interphase of polymer-in-salt electrolyte in all-solid-state lithium batteries, *Energy Mater. Adv.* 2021 (2021) 1932952.
- [17] E. Quartarone, P. Mustarelli, Electrolytes for solid-state lithium rechargeable batteries: Recent advances and perspectives, *Chem. Soc. Rev.* 40 (5) (2011) 2525–2540.
- [18] M.H. Zhou, R.L. Liu, D.Y. Jia, Y. Cui, Q.T. Liu, S.H. Liu, D.C. Wu, Ultrathin yet robust single lithium-ion conducting quasi-solid-state polymer-brush electrolytes enable ultralong-life and dendrite-free lithium-metal batteries, *Adv. Mater.* 33 (29) (2021) 2100943.
- [19] J.H. Li, Y.F. Cai, H.M. Wu, Z. Yu, X.Z. Yan, Q.H. Zhang, T.D.Z. Gao, K. Liu, X. D. Jia, Z.N. Bao, Polymers in lithium-ion and lithium metal batteries, *Adv. Energy Mater.* 11 (15) (2021) 2003239.
- [20] Q. Zhou, J.J. Zhang, G.L. Cui, Rigid-flexible coupling polymer electrolytes toward high-energy lithium batteries, *Macromol. Mater. Eng.* 303 (11) (2018) 1800337.
- [21] L.N. Dong, X.F. Zeng, J.F. Fu, L.Y. Chen, J. Zhou, S.W. Dai, L.Y. Shi, Cross-linked ionic copolymer solid electrolytes with loose Coordination-assisted lithium transport for lithium batteries, *Chem. Eng. J.* 423 (2021), 130209.
- [22] R. Khurana, J.L. Schaefer, L.A. Archer, G.W. Coates, Suppression of lithium dendrite growth using cross-linked polyethylene/poly(ethylene oxide) electrolytes: A new approach for practical lithium-metal polymer batteries, *J. Am. Chem. Soc.* 136 (20) (2014) 7395–7402.
- [23] R. Bouchet, S. Maria, R. Meziane, A. Aboulaich, L. Lienafa, J.P. Bonnet, T.N. T. Phan, D. Bertin, D. Gigmes, D. Devaux, R. Denoyel, M. Armand, Single-ion BAB triblock copolymers as highly efficient electrolytes for lithium-metal batteries, *Nat. Mater.* 12 (5) (2013) 452–457.
- [24] J. Peng, L.N. Wu, J.X. Lin, C.G. Shi, J.J. Fan, L.B. Chen, P. Dai, L. Huang, J.T. Li, S. G. Sun, A solid-state dendrite-free lithium-metal battery with improved electrode interphase and ion conductivity enhanced by a bifunctional solid plasticizer, *J. Mater. Chem. A* 7 (33) (2019) 19565–19572.
- [25] J.H. Cha, P.N. Didwal, J.M. Kim, D.R. Chang, C.J. Park, Poly(ethylene oxide)-based composite solid polymer electrolyte containing  $\text{Li}_7\text{La}_3\text{Zr}_2\text{O}_{12}$  and poly(ethylene glycol) dimethyl ether, *J. Membr. Sci.* 595 (2020), 117538.
- [26] A.J. Blake, R.R. Kohlmeier, J.O. Hardin, E.A. Carmona, B. Maruyama, J. D. Berrigan, H. Huang, M.F. Durstock, 3D printable ceramic-polymer electrolytes for flexible high-performance Li-ion batteries with enhanced thermal stability, *Adv. Energy Mater.* 7 (14) (2017) 1602920.
- [27] D. Zhou, R.L. Liu, Y.B. He, F.Y. Li, M. Liu, B.H. Li, Q.H. Yang, Q. Cai, F.Y. Kang,  $\text{SiO}_2$  hollow nanosphere-based composite solid electrolyte for lithium metal batteries to suppress lithium dendrite growth and enhance cycle life, *Adv. Energy Mater.* 6 (7) (2016) 1502214.
- [28] A.K. Salarajan, V. Murugadoss, S. Angaiah, Dimensional stability and electrochemical behaviour of  $\text{ZrO}_2$  incorporated electrospun PVPF-HFP based nanocomposite polymer membrane electrolyte for Li-ion capacitors, *Sci Rep* 7 (2017) 45390.
- [29] J.C. Bachman, S. Muy, A. Grimaud, H.H. Chang, N. Pour, S.F. Lux, O. Paschos, F. Maglia, S. Lupart, P. Lamp, L. Giordano, Y. Shao-Horn, Inorganic solid-state electrolytes for lithium batteries: mechanisms and properties governing ion conduction, *Chem. Rev.* 116 (1) (2016) 140–162.
- [30] L.Q. Xu, J.Y. Li, W.T. Deng, H.L. Shuai, S. Li, Z.F. Xu, J.H. Li, H.S. Hou, H.J. Peng, G.Q. Zou, X.B. Ji, Garnet solid electrolyte for advanced all-solid-state Li batteries, *Adv. Energy Mater.* 11 (2) (2021) 2000648.
- [31] Z.L. Jian, Y.S. Hu, X.L. Ji, W. Chen, NASICON-structured materials for energy storage, *Adv. Mater.* 29 (20) (2017) 1601925.
- [32] W. Liu, N. Liu, J. Sun, P.C. Hsu, Y.Z. Li, H.W. Lee, Y. Cui, Ionic conductivity enhancement of polymer electrolytes with ceramic nanowire fillers, *Nano Lett.* 15 (4) (2015) 2740–2745.
- [33] D.C. Lin, W. Liu, Y.Y. Liu, H.R. Lee, P.C. Hsu, K. Liu, Y. Cui, High ionic conductivity of composite solid polymer electrolyte via in situ synthesis of

- monodispersed SiO<sub>2</sub> nanospheres in poly(ethylene oxide), *Nano Lett.* 16 (1) (2016) 459–465.
- [34] H. Yang, M.X. Jing, H.P. Li, W.Y. Yuan, B. Deng, Q.Y. Liu, B.W. Ju, X.Y. Zhang, S. Hussain, X.Q. Shen, X.H. Yan, 'Environment-friendly' polymer solid electrolyte membrane via a rapid surface-initiating polymerization strategy, *Chem. Eng. J.* 421 (2021), 129710.
- [35] Y.M. Wang, Z.T. Wang, J.G. Sun, F. Zheng, M. Kotobuki, T. Wu, K.Y. Zeng, L. Lu, Flexible, stable, fast-ion-conducting composite electrolyte composed of nanostructured Na-super-ion-conductor framework and continuous Poly(ethylene oxide) for all-solid-state Na battery, *J. Power Sources* 454 (2020), 227949.
- [36] H.W. Zhai, P.Y. Xu, M.Q. Ning, Q. Cheng, J. Mandal, Y. Yang, A flexible solid composite electrolyte with vertically aligned and connected ion-conducting nanoparticles for lithium batteries, *Nano Lett.* 17 (5) (2017) 3182–3187.
- [37] X. Wang, H.W. Zhai, B.Y. Qie, Q. Cheng, A.J. Li, J. Borovilas, B.Q. Xu, C.M. Shi, T. W. Jin, X.B. Liao, Y.B. Li, X.D. He, S.Y. Du, Y.K. Fu, M. Dontigny, K. Zaghib, Y. Yang, Rechargeable solid-state lithium metal batteries with vertically aligned ceramic nanoparticle/polymer composite electrolyte, *Nano Energy* 60 (2019) 205–212.
- [38] H. Xie, C.P. Yang, K. Fu, Y.G. Yao, F. Jiang, E. Hitz, B.Y. Liu, S. Wang, L.B. Hu, Flexible, scalable, and highly conductive garnet-polymer solid electrolyte templated by bacterial cellulose, *Adv. Energy Mater.* 8 (18) (2018) 1703474.
- [39] J.Q. Dai, K. Fu, Y.H. Gong, J.W. Song, C.J. Chen, Y.G. Yao, G. Pastel, L. Zhang, E. Wachsman, L.B. Hu, Flexible solid-state electrolyte with aligned nanostructures derived from wood, *ACS Mater. Lett.* 1 (3) (2019) 354–361.
- [40] Y. Yang, Z. Wang, Q. He, X. Li, G. Lu, L. Jiang, Y. Zeng, B. Bethers, J. Jin, S. Lin, S. Xiao, Y. Zhu, X. Wu, W. Xu, Q. Wang, Y. Chen, 3D printing of nacre-inspired structures with exceptional mechanical and flame-retardant properties, *Research* 2022 (2022) 9840574.
- [41] L.J. Deiner, C.A.G. Bezerra, T.G. Howell, A.S. Powell, Digital printing of solid-state lithium-ion batteries, *Adv. Energy Mater.* 21 (11) (2019) 1900737.
- [42] X.C. Tian, B.G. Xu, 3D printing for solid-state energy storage, *Small Methods* 5 (12) (2021) 2100877.
- [43] H. Xie, Y.H. Bao, J. Cheng, C.W. Wang, E.M. Hitz, C.P. Yang, Z.A. Liang, Y. B. Zhou, S.M. He, T. Li, L.B. Hu, Flexible garnet solid-state electrolyte membranes enabled by tile-and-grout design, *ACS Energy Lett.* 4 (11) (2019) 2668–2674.
- [44] S. Zekoll, C. Marriner-Edwards, A.K.O. Hekselman, J. Kasemchainan, C. Kuss, D. E.J. Armstrong, D.Y. Cai, R.J. Wallace, F.H. Richter, J.H.J. Thijssen, P.G. Bruce, Hybrid electrolytes with 3D bicontinuous ordered ceramic and polymer microchannels for all-solid-state batteries, *Energy Environ. Sci.* 11 (1) (2018) 185–201.
- [45] Q.L. Wei, F.Y. Xiong, S.S. Tan, L. Huang, E.H. Lan, B. Dunn, L.Q. Mai, Porous one-dimensional nanomaterials: design, fabrication and applications in electrochemical energy storage, *Adv. Mater.* 29 (20) (2017) 1602300.
- [46] F.Z. Zhang, P.C. Sherrell, W. Luo, J. Chen, W. Li, J.P. Yang, M.F. Zhu, Organic/inorganic hybrid fibers: controllable architectures for electrochemical energy applications, *Adv. Sci.* 8 (22) (2021) 2102859.
- [47] Y.T. Wang, H. Wu, D.D. Lin, R. Zhang, H.P. Li, W. Zhang, W. Liu, S.Y. Huang, L. Yao, J. Cheng, M. Shahid, M.F. Zhang, T. Suzuki, W. Pan, One-dimensional zirconium ceramic nanomaterials and their sensing applications, *J. Am. Ceram. Soc.* 105 (2) (2022) 765–785.
- [48] C.J. Niu, J.S. Meng, X.P. Wang, C.H. Han, M.Y. Yan, K.N. Zhao, X.M. Xu, W. H. Ren, Y.L. Zhao, L. Xu, Q.J. Zhang, D.Y. Zhao, L.Q. Mai, General synthesis of complex nanotubes by gradient electrospinning and controlled pyrolysis, *Nat. Commun.* 6 (2015) 7402.
- [49] Y.J. Hong, J.W. Yoon, J.H. Lee, Y.C. Kang, A new concept for obtaining SnO<sub>2</sub> fiber-in-tube nanostructures with superior electrochemical properties, *Chem. Eur. J.* 21 (1) (2015) 371–376.
- [50] L.C. Yue, H.T. Zhao, Z.G. Wu, J. Liang, S.Y. Lu, G. Chen, S.Y. Gao, B.H. Zhong, X. D. Guo, X.P. Sun, Recent advances in electrospun one-dimensional carbon nanofiber structures/heterostructures as anode materials for sodium ion batteries, *J. Mater. Chem. A* 8 (23) (2020) 11493–11510.
- [51] J.J. Xue, T. Wu, Y.Q. Dai, Y.N. Xia, Electrospinning and electrospun nanofibers: methods, materials, and applications, *Chem. Rev.* 119 (8) (2019) 5298–5415.
- [52] J. Sharma, G. Polizo, C.J. Jafta, D.L. Wood, J.L. Li, Review-electrospun inorganic solid-state electrolyte fibers for battery applications, *J. Electrochem. Soc.* 169 (5) (2022), 050527.
- [53] K. Fu, Y.H. Gong, J.Q. Dai, A. Gong, X.G. Han, Y.G. Yao, C.W. Wang, Y.B. Wang, Y.N. Chen, C.Y. Yan, Y.J. Li, E.D. Wachsman, L.B. Hu, Flexible, solid-state, ion-conducting membrane with 3D garnet nanofiber networks for lithium batteries, *Proc. Natl. Acad. Sci. U. S. A.* 113 (26) (2016) 7094–7099.
- [54] J.M. Yu, C. Wang, S.H. Li, N. Liu, J. Zhu, Z.D. Lu, Li<sup>+</sup>-containing, continuous silica nanofibers for high Li<sup>+</sup> conductivity in composite polymer electrolyte, *Small* 15 (44) (2019) 1902729.
- [55] J. Bae, Y.T. Li, J. Zhang, X.Y. Zhou, F. Zhao, Y. Shi, J.B. Goodenough, G.H. Yu, A 3D nanostructured hydrogel-framework-derived high-performance composite polymer lithium-ion electrolyte, *Angew. Chem. Int. Edit.* 57 (8) (2018) 2096–2100.
- [56] J. Bae, Y.T. Li, F. Zhao, X.Y. Zhou, Y. Ding, G.H. Yu, Designing 3D nanostructured garnet frameworks for enhancing ionic conductivity and flexibility in composite polymer electrolytes for lithium batteries, *Energy Storage Mater.* 15 (2018) 46–52.
- [57] X. Judez, H. Zhang, C.M. Li, G.G. Eshetu, J.A. Gonzalez-Marcos, M. Armand, L. M. Rodriguez-Martinez, Review-solid electrolytes for safe and high energy density lithium-sulfur batteries: Promises and challenges, *J. Electrochem. Soc.* 165 (1) (2018) A6008–A6016.
- [58] A.M. Stephan, Review on gel polymer electrolytes for lithium batteries, *Eur. Polym. J.* 42 (1) (2006) 21–42.
- [59] Y. Liu, B. Xu, W. Zhang, L. Li, Y. Lin, C. Nan, Composition modulation and structure design of inorganic-in-polymer composite solid electrolytes for advanced lithium batteries, *Small* 16 (15) (2020) 1902813.
- [60] Z.G. Xue, D. He, X.L. Xie, Poly(ethylene oxide)-based electrolytes for lithium-ion batteries, *J. Mater. Chem. A* 3 (38) (2015) 19218–19253.
- [61] P. Hu, J.C. Chai, Y.L. Duan, Z.H. Liu, G.L. Cui, L.Q. Chen, Progress in nitrile-based polymer electrolytes for high performance lithium batteries, *J. Mater. Chem. A* 4 (26) (2016) 10070–10083.
- [62] L.N. Sim, F.C. Sentanin, A. Pawlicka, R. Yahya, A.K. Arof, Development of polyacrylonitrile-based polymer electrolytes incorporated with lithium bis (trifluoromethane)sulfonimide for application in electrochromic device, *Electrochim. Acta* 229 (2017) 22–30.
- [63] R. Hussain, D. Mohammad, X-ray diffraction study of the changes induced during the thermal degradation of poly (methyl methacrylate) and poly (methacryloyl chloride), *Turk. J. Chem.* 28 (6) (2004) 725–729.
- [64] N. Shukla, A.K. Thakur, Role of salt concentration on conductivity optimization and structural phase separation in a solid polymer electrolyte based on PMMA-LiClO<sub>4</sub>, *Ionics* 15 (3) (2009) 357–367.
- [65] C.Y. Wan, C.R. Bowen, Multiscale-structuring of polyvinylidene fluoride for energy harvesting: the impact of molecular-, micro- and macro-structure, *J. Mater. Chem. A* 5 (7) (2017) 3091–3128.
- [66] X. Zhang, S. Wang, C.J. Xue, C.Z. Xin, Y.H. Lin, Y. Shen, L.L. Li, C.W. Nan, Self-suppression of lithium dendrite in all-solid-state lithium metal batteries with poly (vinylidene difluoride)-based solid electrolytes, *Adv. Mater.* 31 (11) (2019) 1806082.
- [67] Y. Liu, P. He, H. Zhou, Rechargeable solid-state Li-air and Li-S batteries: Materials, construction, and challenges, *Adv. Energy Mater.* 8 (4) (2018) 1701602.
- [68] Y. Inaguma, C. Liqun, M. Itoh, T. Nakamura, T. Uchida, H. Ikuta, M. Wakihara, High ionic conductivity in lithium lanthanum titanate, *Solid State Communications* 86 (10) (1993) 689–693.
- [69] O. Bohnke, C. Bohnke, J.L. Fourquet, Mechanism of ionic conduction and electrochemical intercalation of lithium into the perovskite lanthanum lithium titanate, *Solid State Ionics* 91 (1) (1996) 21–31.
- [70] C.R. Mariappan, C. Yada, F. Rosciano, B. Roling, Correlation between micro-structural properties and ionic conductivity of Li<sub>1.5</sub>Al<sub>0.5</sub>Ge<sub>1.5</sub>(PO<sub>4</sub>)<sub>3</sub> ceramics, *J. Power Sources* 196 (15) (2011) 6456–6464.
- [71] B. Kumar, D. Thomas, J. Kumar, Space-charge-mediated superionic transport in lithium ion conducting glass-ceramics, *J. Electrochem. Soc.* 156 (7) (2009) A506.
- [72] B.H. Zhang, Y.L. Liu, J. Liu, L.Q. Sun, L.N. Cong, F. Fu, A. Mauger, C.M. Julien, H. M. Xie, X.M. Pan, "Polymer-in-ceramic" based poly(ε-caprolactone)/ceramic composite electrolyte for all-solid-state batteries, *J. Energy Chem.* 52 (2021) 318–325.
- [73] D. Rettenwander, G. Redhammer, F. Preishuber-Pflügl, L. Cheng, L. Miara, R. Wagner, A. Welzl, E. Suard, M.M. Doeff, M. Wilkening, J. Fleig, G. Amthauer, Structural and electrochemical consequences of Al and Ga substitution in Li<sub>7</sub>La<sub>3</sub>Zr<sub>2</sub>O<sub>12</sub> solid electrolytes, *Chem. Mater.* 28 (7) (2016) 2384–2392.
- [74] C. Bernuy-Lopez, W. Manalastas, J.M.L. del Amo, A. Agudero, F. Aguesse, J. A. Kilner, Atmosphere controlled processing of Ga-substituted garnets for high Li-ion conductivity ceramics, *Chem. Mater.* 26 (12) (2014) 3610–3617.
- [75] S. Ohta, T. Kobayashi, T. Asaoka, High lithium ionic conductivity in the garnet-type oxide Li<sub>7-x</sub>La<sub>3</sub>(Zr<sub>2-x</sub>Nb<sub>x</sub>)O<sub>12</sub> (X=0-2), *J. Power Sources* 196 (6) (2011) 3342–3345.
- [76] R. Jaleem, M.J.D. Rushton, W. Manalastas, M. Nakayama, T. Kasuga, J.A. Kilner, R.W. Grimes, Effects of gallium doping in garnet-type Li<sub>7</sub>La<sub>3</sub>Zr<sub>2</sub>O<sub>12</sub> solid electrolytes, *Chem. Mater.* 27 (8) (2015) 2821–2831.
- [77] N. Kamaya, K. Homma, Y. Yamakawa, M. Hirayama, R. Kanno, M. Yonemura, T. Kamiyama, Y. Kato, S. Hama, K. Kawamoto, A. Mitsui, A lithium superionic conductor, *Nat. Mater.* 10 (9) (2011) 682–686.
- [78] S. Wang, Y.B. Zhang, X. Zhang, T. Liu, Y.H. Lin, Y. Shen, L.L. Li, C.W. Nan, High-conductivity argyrodite Li<sub>6</sub>PS<sub>3</sub>Cl solid electrolytes prepared via optimized sintering processes for all-solid-state lithium-sulfur batteries, *ACS Appl. Mater. Interfaces* 10 (49) (2018) 42279–42285.
- [79] T. Ohtomo, A. Hayashi, M. Tatsumisago, Y. Tsuchida, S. Hama, K. Kawamoto, All-solid-state lithium secondary batteries using the 75Li<sub>2</sub>S·25P<sub>2</sub>S<sub>5</sub> glass and the 70Li<sub>2</sub>S·30P<sub>2</sub>S<sub>5</sub> glass-ceramic as solid electrolytes, *J. Power Sources* 233 (2013) 231–235.
- [80] Q.W. Pan, D.M. Smith, H. Qi, S.J. Wang, C.Y. Li, Hybrid electrolytes with controlled network structures for lithium metal batteries, *Adv. Mater.* 27 (39) (2015) 5995–6001.
- [81] F. Croce, G.B. Appetecchi, L. Persi, B. Scrosati, Nanocomposite polymer electrolytes for lithium batteries, *Nature* 394 (6692) (1998) 456–458.
- [82] Y. Lin, X.M. Wang, J. Liu, J.D. Miller, Natural halloysite nano-clay electrolyte for advanced all-solid-state lithium-sulfur batteries, *Nano Energy* 31 (2017) 478–485.
- [83] J. Shim, H.J. Kim, B.G. Kim, Y.S. Kim, D.G. Kim, J.C. Lee, 2D boron nitride nanoflakes as a multifunctional additive in gel polymer electrolytes for safe, long cycle life and high rate lithium metal batteries, *Energy Environ. Sci.* 10 (9) (2017) 1911–1916.
- [84] X.K. Zhang, J. Xie, F.F. Shi, D.C. Lin, Y.Y. Liu, W. Liu, A. Pei, Y.J. Gong, H. X. Wang, K. Liu, Y. Xiang, Y. Cui, Vertically aligned and continuous nanoscale ceramic-polymer interfaces in composite solid polymer electrolytes for enhanced ionic conductivity, *Nano Lett.* 18 (6) (2018) 3829–3838.

- [85] J.G. Sun, Q.M. Sun, A. Plewa, Y.M. Wang, L.C. He, F. Zheng, C. Chen, W. Zajac, J. Molenda, K.Y. Zeng, L. Lu, Abnormal ionic conductivities in halide  $\text{NaBi}_3\text{O}_4\text{Cl}_2$  induced by absorbing water and derived oxyhydril group, *Angew. Chem. Int. Ed.* 59 (2020) 8991.
- [86] N. Wu, P.-H. Chien, Y.M. Qian, Y.T. Li, H.H. Xu, N.S. Grundish, B.Y. Xu, H.B. Jin, Y.-Y. Hu, G.H. Yu, J.B. Goodenough, Enhanced surface interactions enable fast  $\text{Li}^+$  conduction in oxide/polymer composite electrolyte, *Angew. Chem. Int. Ed.* 59 (2020) 4131.
- [87] Y.M. Wang, Z.T. Wang, F. Zheng, J.G. Sun, J.A.S. Oh, T. Wu, G.X. Chen, Q. Huang, M. Kotobuki, K.Y. Zeng, L. Lu, Ferroelectric engineered electrode-composite polymer electrolyte interfaces for all-solid-state sodium metal battery, *Adv. Sci.* 9 (2022) 2105849.
- [88] H. Yamada, A.J. Bhattacharyya, J. Maier, Extremely high silver ionic conductivity in composites of silver halide (AgBr, AgI) and mesoporous alumina, *Adv. Funct. Mater.* 16 (4) (2006) 525–530.
- [89] Z. Li, H.-M. Huang, J.-K. Zhu, J.-F. Wu, H. Yang, L. Wei, X. Guo, Ionic conduction in composite polymer electrolytes: case of PEO:Ga-LLZO composites, *ACS Appl. Mater. Interfaces* 11 (1) (2019) 784–791.
- [90] Y. Cheng, J. Shu, L. Xu, Y.Y. Xia, L.L. Du, G. Zhang, L.Q. Mai, Flexible nanowire cathode membrane with gradient interfaces and rapid electron/ion transport channels for solid-state lithium batteries, *Adv. Energy Mater.* 11 (12) (2021) 2100026.
- [91] S. Hu, L.L. Du, G. Zhang, W.Y. Zou, Z. Zhu, L. Xu, L.Q. Mai, Open-structured nanotubes with three-dimensional ion-accessible pathways for enhanced  $\text{Li}^+$  conductivity in composite solid electrolytes, *ACS Appl. Mater. Interfaces* 13 (11) (2021) 13183–13190.
- [92] W.J. Tang, S. Tang, C.J. Zhang, Q.T. Ma, Q. Xiang, Y.W. Yang, J.Y. Luo, Simultaneously enhancing the thermal stability, mechanical modulus, and electrochemical performance of solid polymer electrolytes by incorporating 2D sheets, *Adv. Energy Mater.* 8 (24) (2018) 1800866.
- [93] D. Li, L. Chen, T.S. Wang, L.Z. Fan, 3D fiber-network-reinforced bicontinuous composite solid electrolyte for dendrite-free lithium metal batteries, *ACS Appl. Mater. Interfaces* 10 (8) (2018) 7069–7078.
- [94] J.Y. Bi, D.B. Mu, B.R. Wu, J.L. Fu, H. Yang, G. Mu, L. Zhang, F. Wu, A hybrid solid electrolyte  $\text{Li}_{0.33}\text{La}_{0.557}\text{TiO}_3/\text{poly}(\text{acrylonitrile})$  membrane infiltrated with a succinonitrile-based electrolyte for solid state lithium-ion batteries, *J. Mater. Chem. A* 8 (2) (2020) 706–713.
- [95] Y.H. Gong, K. Fu, S.M. Xu, J.Q. Dai, T.R. Hamann, L. Zhang, G.T. Hitz, Z.Z. Fu, Z. H. Ma, D.W. McOwen, X.G. Han, L.B. Hu, E.D. Wachsman, Lithium-ion conductive ceramic textile: A new architecture for flexible solid-state lithium metal batteries, *Mater. Today* 21 (6) (2018) 594–601.
- [96] P. Pan, M.M. Zhang, Z.L. Cheng, L.Y. Jiang, J.T. Mao, C.K. Ni, Q. Chen, Y. Zeng, Y. Hu, K. Fu, Garnet ceramic fabric-reinforced flexible composite solid electrolyte derived from silk template for safe and long-term stable All-Solid-State lithium metal batteries, *Energy Storage Mater.* 47 (2022) 279–287.
- [97] L.L. Du, B. Zhang, W. Deng, Y. Cheng, L. Xu, L.Q. Mai, Hierarchically self-assembled MOF network enables continuous ion transport and high mechanical strength, *Adv. Energy Mater.* 12 (2022) 2200501.
- [98] J.M. Yu, T.L. Guo, C. Wang, Z.H. Shen, X.Y. Dong, S.H. Li, H.G. Zhang, Z.D. Lu, Engineering two-dimensional metal-organic framework on molecular basis for fast  $\text{Li}^+$  conduction, *Nano Lett.* 21 (13) (2021) 5805–5812.
- [99] Y.Y. Hu, R.X. Han, L. Mei, J.L. Liu, J.C. Sun, K. Yang, J.W. Zhao, Design principles of MOF-related materials for highly stable metal anodes in secondary metal-based batteries, *Mater. Today Energy* 19 (2021), 100608.
- [100] C. Wang, D.F. Huang, S.H. Li, J.M. Yu, M.W. Zhu, N. Liu, Z.D. Lu, Three-dimensional-percolated ceramic nanoparticles along natural-cellulose-derived hierarchical networks for high  $\text{Li}^+$  conductivity and mechanical strength, *Nano Lett.* 20 (10) (2020) 7397–7404.
- [101] M.M. Zhang, P. Pan, Z.L. Cheng, J.T. Mao, L.Y. Jiang, C.K. Ni, S.K. Park, K. Y. Deng, Y. Hu, K.K. Fu, Flexible, mechanically robust, solid-state electrolyte membrane with conducting oxide-enhanced 3D nanofiber networks for lithium batteries, *Nano Lett.* 21 (16) (2021) 7070–7078.
- [102] W.J. Tang, S. Tang, X.Z. Guan, X.Y. Zhang, Q. Xiang, J.Y. Luo, High-performance solid polymer electrolytes filled with vertically aligned 2D materials, *Adv. Funct. Mater.* 29 (16) (2019) 1900648.
- [103] J.Y. Wan, J. Xie, X. Kong, Z. Liu, K. Liu, F.F. Shi, A. Pei, H. Chen, W. Chen, J. Chen, X.K. Zhang, L.Q. Zong, J.Y. Wang, L.Q. Chen, J. Qin, Y. Cui, Ultrathin, flexible, solid polymer composite electrolyte enabled with aligned nanoporous host for lithium batteries, *Nat. Nanotechnol.* 14 (7) (2019) 705–711.
- [104] D.C. Lin, P.Y. Yuen, Y.Y. Liu, W. Liu, N. Liu, R.H. Dauskardt, Y. Cui, A silica-aerogel-reinforced composite polymer electrolyte with high ionic conductivity and high modulus, *Adv. Mater.* 30 (32) (2018) 1802661.
- [105] Y. Cui, J.Y. Wan, Y.S. Ye, K. Liu, L.Y. Chou, A fireproof, lightweight, polymer-polymer solid-state electrolyte for safe lithium batteries, *Nano Lett.* 20 (3) (2020) 1686–1692.
- [106] C.F. Ding, X.W. Fu, H. Li, J.Y. Yang, J.L. Lan, Y.H. Yu, W.H. Zhong, X.P. Yang, An ultrarobust composite gel electrolyte stabilizing ion deposition for long-life lithium metal batteries, *Adv. Funct. Mater.* 29 (43) (2019) 1904547.
- [107] Z. Li, W.X. Sha, X. Guo, Three-dimensional garnet framework-reinforced solid composite electrolytes with high lithium-ion conductivity and excellent stability, *ACS Appl. Mater. Interfaces* 11 (30) (2019) 26920–26927.
- [108] X. Peng, K. Huang, S.P. Song, F. Wu, Y. Xiang, X.K. Zhang, Garnet-polymer composite electrolytes with high  $\text{Li}^+$  conductivity and transference number via well-fused grain boundaries in microporous frameworks, *ChemElectroChem* 7 (11) (2020) 2389–2394.
- [109] A.J. Li, X.B. Liao, H.R. Zhang, L. Shi, P.Y. Wang, Q. Cheng, J. Borovilas, Z.Y. Li, W.L. Huang, Z.X. Fu, M. Dontigny, K. Zaghib, K. Myers, X.Y. Chuan, X. Chen, Y. Yang, Nacre-inspired composite electrolytes for load-bearing solid-state lithium-metal batteries, *Adv. Mater.* 32 (2) (2020) 1905517.
- [110] Q.W. Lu, Y.B. He, Q.P. Yu, B.H. Li, Y.V. Kaneti, Y.W. Yao, F.Y. Kang, Q.H. Yang, Dendrite-free, high-rate, long-life lithium metal batteries with a 3D cross-linked network polymer electrolyte, *Adv. Mater.* 1604460 (2017).
- [111] Y.H. Zhu, J. Cao, H. Chen, Q.P. Yua, B.H. Li, High electrochemical stability of a 3D cross-linked network PEO@nano- $\text{SiO}_2$  composite polymer electrolyte for lithium metal batteries, *J. Mater. Chem. A* 7 (2019) 6832–6839.
- [112] J.Y. Liang, R.M. Tao, J. Tu, C. Guo, K. Du, R. Guo, W. Zhang, X.L. Liu, P.M. Guo, D.Y. Wang, S. Dai, X.G. Sun, Design of a multi-functional gel polymer electrolyte with a 3D compact stacked polymer micro-sphere matrix for high-performance lithium metal batteries, *J. Mater. Chem. A* 10 (2022) 12563–12574.
- [113] X.R. Zuo, Y. Cheng, L. Xu, R.P. Chen, F. Liu, H. Zhang, L.Q. Mai, A novel thioctic acid-functionalized hybrid network for solid-state batteries, *Energy Storage Mater.* 46 (2022) 570–576.